

Marine Actinomycetes Siderophores: Types, High Throughput Characterization Techniques, Applications, and Their Association with Nanotechnology: A Comprehensive Review

Mounika Sarvepalli¹, Aditya Velidandi¹, Arun Kumar Ramachandravarapu² and Narasimhulu Korrapati¹

¹Department of Biotechnology, National Institute of Technology, Warangal, Telangana, India

²Department of Biochemistry and Bioinformatics, GITAM University, Vishakhapatnam, Andhra Pradesh, India

*Correspondence to:

Mounika Sarvepalli
Department of Biotechnology,
National Institute of Technology,
Warangal, Telangana, India.
E-mail: mouni.sarvepalli@gmail.com

Received: January 05, 2024

Accepted: February 08, 2024

Published: February 12, 2024

Citation: Sarvepalli M, Velidandi A, Ramachandravarapu AK, Korrapati N. 2024. Marine Actinomycetes Siderophores: Types, High Throughput Characterization Techniques, Applications, and Their Association with Nanotechnology: A Comprehensive Review. *NanoWorld J* 10(1): 1-21.

Copyright: © 2024 Sarvepalli et al. This is an Open Access article distributed under the terms of the Creative Commons Attribution 4.0 International License (CC-BY) (<http://creativecommons.org/licenses/by/4.0/>) which permits commercial use, including reproduction, adaptation, and distribution of the article provided the original author and source are credited.

Published by United Scientific Group

Abstract

Iron is one of the most essential micronutrients for all the existing life systems. However, at biological pH, iron gets oxidised to insoluble oxyhydroxide polymers. In low iron conditions, microbes secrete specialised molecules called siderophores, which are high affinity and low molecular weight chelating agents that increase the availability of iron for microbial usage. In marine water, concentration of iron is as low as nanomolar. Very less light has been shed on the siderophores of marine actinomycetes. Actinomycetes are known for producing novel secondary metabolites with diverse biological activities, siderophores are one such bioactive metabolite. Siderophores significantly differs in structure based on the ligands of oxygen for iron(III) (Ferric, Fe⁺³) synchronization. The applications of siderophores include heavy metal remediation, treating metal toxicity. In medical field, they are employed to treat diseases like thalassemia, sickle cell anaemia, and used to treat few cancers. They are being exploited to combat antibiotic-resistant bacteria, which is a mounting problem these days. It has been reported that they can also be used as biosensors for iron detection. Recently developed high throughput strategies, HPLC-MS and MS/MS methods are used to identify and quantify many unknown siderophores. In this review, recent developments, and diverse applications of marine siderophores are reported. The review also highlights the association and involvement of siderophores in the synthesis of various NPs and their applications in the fields of medical to environmental biotechnology.

Keywords

Marine siderophores, Actinomycetes, Nanoparticles, Biosensors, Heavy metal chelation, Ion sensing

Abbreviations

ACN: Acetonitrile; ATP: Adenosine triphosphate; CAS: Chrome azurol S; CD: Circular dichroism; CI-MS: Chemical ionization mass spectrometry; DFO: Desferrioxamine; DNA: Deoxyribonucleic acid; DOX: Doxorubicin; FAB MS: Fast atom bombardment mass spectrometry; FTICR-MS: Fourier transform ion cyclotron resonance mass spectrometry; GC-MS: Gas chromatography mass spectrometry; HPLC: High performance liquid chromatography; HR-ESI-MS: High resolution electrospray ionization mass spectrometry; HRMS: High resolution mass spectrometry; ICPMS: Inductively coupled plasma mass spectrometry; ID: Internal diameter; MALDI: Matrix-assisted laser desorption/ionization; MS: Mass spectrometry; m/z: Mass/charge ratio; NMR: Nuclear magnetic resonance; NPs: Nanoparticles; PGPB: Plant growth promoting bacteria; PVD: Pyoverdine; QCM: Quartz crystal microbalance; Q-TOF: Quadrupole-time of flight;

SI-MS: Secondary ion mass spectrometry; SPIONs: super-paramagnetic iron oxide NPs; and TFA: Trifluoroacetic acid.

Introduction

Iron is an essential micronutrient for most of the growth and developmental processes of every living being (Figure 1) [1]. Under aerobic conditions, microbes require iron for the reduction of oxygen, synthesis of ATP, reduction of ribonucleotide precursors of DNA, formation of heme, in the electron transport chain, and as a cofactor for many enzymes [2, 3]. In nature, the solubility of Fe^{+3} is 10^{-17} M at neutrality, but certain microorganisms like bacterium need 10^{-5} to 10^{-7} M for their optimal growth [4]. Though, iron being the fourth most common element on earth's crust, it is inaccessible to microbes because formation of precipitates of oxyhydroxide polymers by oxidation. In oceans, 0.01 to 2 nM concentration of iron present in the surface water but micromolar levels of iron is required for marine microbes [5, 6]. So, to survive under iron starvation conditions, bacteria living in the soil and water should have a mechanism to solubilize and transport iron from precipitates for their growth and energy needs.

In counter to the above problem, microbes adopted a strategy to secrete certain organic molecules called "siderophores" (in Greek, sidero means iron, phores means carrier) which are high affinity and low molecular weight (< 10 KDa) metal chelating agents [7, 8]. Currently, academic, and pharmaceutical industry are interested towards marine microorganisms, as they became an important source to produce industrially important molecules which are unique and biologically active molecules have been reported till now [9-11].

Actinomycetes have a broad spectrum of ecological habitats like terrestrial, compost, sewage, fresh water, lake, back-water, and marine environment. Actinomycetes are high G + C Gram-positive, aerobic bacteria and distinctive in forming branching filaments (hyphae) and produce asexual spores. Most of the actinomycetes are non-motile and motility confined to flagellated spores only. They produce antibiotics and various therapeutically important compounds with diverse biological activities and hence considered as highly valuable and can decompose diverse and huge number of organic compounds and play an important role in mineralization of organic matter. Most metabolites have been isolated from actinomycetes about 70% followed by fungi 20%, *Bacillus* 7%,

and *Pseudomonas* 1 to 2%. From the available reports, it is well understood that Actinomycetes are the most important group of microbes studied for the discovery of novel drugs and the identification of bioactive metabolites program [12]. They are mostly available in drier and alkaline soils than waterlogged and acidic soils. Actinomycetes are classified as bacteria, though they are having fungal-like structure and growth [13].

Siderophores

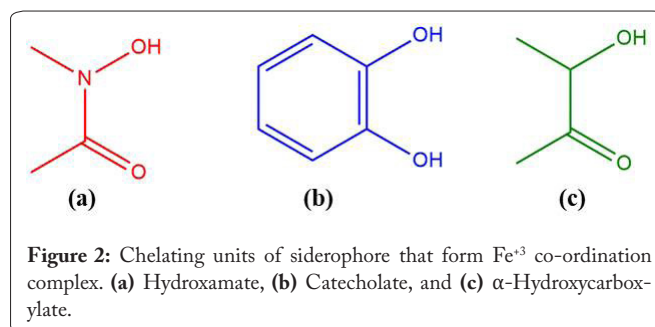
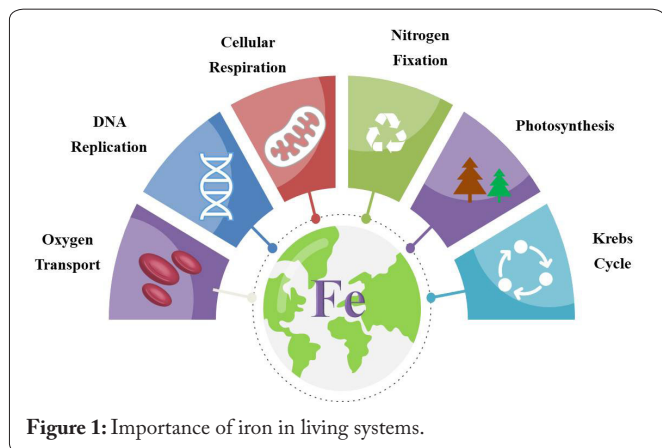
Initially, siderophores were identified as growth factors i.e., myobactin, ferrichrome, and coprogen in 1949 to 1952 [14-16]. Garibaldi and Neilands observed the mode of action of above growth factors and improved the production of ferrichrome A by inoculating the siderophore producing organism in iron deficient media was reported [17]. In 1960's, the Neiland's laboratory scientists formed a natural product group from ETH, Zurich, and Ciba, identified the ferrioxamines, ferrimycin and reported the structural explanation of DFO B. Emery and Neilands elucidated the structures of ferrichrome and ferrichrome A. Presently, more than 500 siderophores are known among them 270 are structurally characterized [18, 19].

Types of Siderophores

The classification of siderophores may include the: (i) Nature of backbone i.e., peptide or nonpeptide and open or close chain, (ii) Nature of the chelating group, (iii) Producing organism, and (iv) Depending on the oxygen ligands for Fe^{+3} coordination [20], siderophores can be classified into three main categories, namely, hydroxamates, catecholates, and α -hydroxycarboxylates (Figure 2).

Hydroxamates

Hydroxamates are commonly found in a group of siderophores an environment that consists of hydroxylated and acylated alkylamines includes N6-acyl-N6-Hydroxy lysine or N5acyl-N5-Hydroxy ornithine in bacteria. This type of siderophore contains C (=O) N-(OH) R, (R = an amino acid or a derivative of it). Marine bacteria were reported to produce suits of amphiphilic siderophores from different genera of bacteria but unique peptide head group to coordinate with Fe^{+3} are amphibactins and marinobactins [21]. *Vibrio* sp. R-10 produced amphibactins having long fatty acid appendages (C14 to C18) which are unsaturated, saturated, hydroxylated, and short peptide head group. Alike mycobactins, these are cell-associated [22]. The marine bacterium *Marinobacter*



sp. DS40M6 produced a group of marinobactins A-E comprise the same six amino acid peptidic head group but differs in the length of the fatty acid appendage (C12 to C16) at N terminus [23]. The marinobactins differ from amphibactins in peptide head (six vs four) and fatty acid tails [22]. Each hydroxamate group of peptide head forms a hexadentate octahedral complex with iron with binding constants in the range of 10^{22} to 10^{32} M⁻¹ [1]. The hydroxamates can be detected by using several methods, initially Neilands assay (spectroscopic) used for finding the production of siderophores. Csaky's assay also widely used to characterize the siderophores. To detect the structure of hydroxamate siderophore ESI-MS has been used [24].

Catecholates

Catecholates are produced by certain bacteria [25]. The catecholate and the hydroxyl group of siderophore coordinate with Fe⁺³ to form a hexadentate octahedral complex. Complex stability, resistance to natural pH, and lipophilicity are catecholate unique properties. Nigribactin a novel siderophore produced from marine bacteria *Vibrio nigripulchritudo*. Structural elucidation reveals the similarity with siderophores vibriobactin and fluvibactin. Nigribactin increases the expression of *spa* encoding protein A by inducing *spa* transcription [26]. This type of siderophore can be detected by Neilands assay, forms wine-coloured complex when siderophore binds FeCl₃ and shows maximum absorbance at 495 nm. O-CAS assay, another method to detect catechol siderophore [27]. The HPLC analysis with diode array detection and ESI-MS assay can be used to detect catecholate siderophore [24].

α-Hydroxycarboxylates

This type of siderophore has both hydroxyl and carboxyl groups that coordinate with iron. A unique property of hydroxycarboxylates is their amphiphilic nature. The aquachelins produced by *Halomonas aquamarina* strain DS40M3, consists of peptide head group and hydrophobic fatty acid tails, forms self-assembled structures because of their amphiphilic and surface-active nature [28]. Loihichelins A-F were derived from the marine *Halomonas* sp. LOB-5 consists of a hydrophilic head group (an octapeptide) and joined by a series of fatty acids ranging from decanoic acid to tetra-decanoic acid. An interesting characteristic of the loihichelins is photoreactive, which relates to the presence of β-hydroxy aspartic acid, which when coordinated to Fe⁺³ [29]. Carboxylates can be detected by spectrophotometric test at 19 to 280 nm [30]. O-CAS assay can be used for the detection of siderophore [27]. In recent times, it has been reported that HPLC and MS are used for structural analysis.

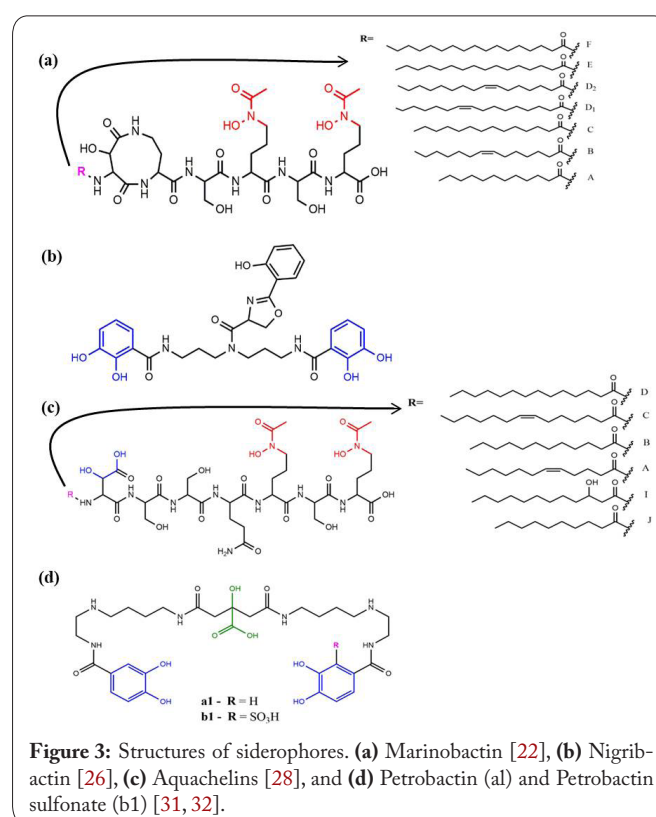
Mixed siderophores

In this type of siderophores, the compound will have a combination of hydroxy, carboxy and catecholates groups inside chains. Petrobactin, a bis-catechol α-hydroxy acid siderophore produced from *Marinobacter hydrocarbonoclasticus* oil-degrading marine bacteria. It is the first report that demonstrates structural characterization and photo decarboxylation when siderophores bound to Fe⁺³. The citryl moiety of

petrobactin binds to iron and found to be quickly photolyzed under sunlight and near-surface sea water. This results in the decarboxylation of α-hydroxy acids and oxidation of petrobactin-iron ligand [4, 31].

Hickford et al. reported a novel siderophore, Petrobactin sulfonate isolated from *M. hydrocarbonoclasticus* contains sulfonated 3,4-dihydroxy aromatic ring. The structure appears in the form of double zwitterion involving N-2 and N-2' and the carboxylate and sulfonate moieties. Petrobactin sulfonate is more hydrophilic than petrobactin due to the presence of sulfonate, which resulted in the short retention times in HPLC [32]. Few structures of different siderophores are shown in figure 3.

Marine *Pseudoalteromonas* sp. KP20-4 bacterium isolated from the Republic of Palau reported producing new siderophores, Pseudoalterobactin A and B. The structure of these compounds is like alterobactins, that have a catechol and two β-hydroxy-Asp residues which have a high affinity towards Fe⁺³ (affinity constant of 10^{49} to 10^{53}). Pseudoalterobactins showed high activity like enterobactin and desferrioxamine B by CAS assay that exhibited 20 μM under assay conditions whereas, enterobactin and desferrioxamine B showed ED50 values of 500 μM and 60 μM, respectively [33].



Siderophores from Marine Actinomycetes

Recently, many siderophores have been isolated from marine bacteria including *Actinomycetes*. *Streptomyces* group of organisms well known for its production of numerous siderophores, which act contingently and regulated independently to compete efficiently in the environment. *Streptomyces* are highly available and important group of actinomycetes in the ma-

rine environment [34]. You et al. isolated 94 different strains of actinomycetes from the marine sediments, among them 87.2% are *Streptomyces* and most of the strains having siderophore producing ability on CAS agar plates and influence the growth of pathogenic *Vibrio* sp. Strains *in vitro* *Streptomyces* can form desiccation-heat resistant spores and probiotic products will be stable under preservation [35]. Streptobactin, a novel catecholate type of siderophore was isolated from actinomycetes *Streptomyces* sp. YM5-799 by chromatography under acidic conditions using porous-polymer resin Diaion HP20 column. Streptobactin (C₅₁H₆₉N₁₅O₁₈) is a colourless gum, having catechol bonded arginine-substituted siderophore framed on a cyclic triester backbone of threonine (-Thr-Arg-DHBA). Along with streptobactin, dibenarthin, tribenarthin, and benarthin were also obtained. When the compounds screened for iron-chelating activity, results showed slightly stronger activity than DFO mesylate. Under iron limited conditions, these siderophores might play a significant role in the existence of *Streptomyces* sp. strain YM5-799 [36].

Nocardamine, a cyclic siderophore isolated from novel marine actinomycete *Citricoccus* sp. KMM3890 from bottom sediments of Sakhalin seashore. It contains three units of 5-succinylated-1-amino-hydroxyamino-pentane which is like bisucaberin-symmetric cyclic dihydroxamate, which was isolated from a marine *Alteromonas haloplanktis*. Initially, nocardamine reported as an antibiotic [37]. Nocardamine was examined for its cytotoxicity to melanoma SK-Mel-5, RPMI-7951, SK-Mel-28, and breast cancer T-47D cell lines *in vitro* using MTS assay and inhibition of colony formation using soft agar clonogenic assay. Results showed no cytotoxicity was observed but nocardamine inhibited colony formation of cancer cells [38].

In silico analysis of marine *Salinispora arenicola* and *S. tropica* proposed that they have several phenolate and hydroxamate type siderophore biosynthetic loci, DFO-B and DFO-E are produced from *Salinispora* in the laboratory. Ejje et al. reported possibility of the biosynthesis of siderophores by genome analysis of marine actinomycete *S. tropica* CNB-440 but unable to predict the siderophore of hydroxamate and phenolate-thia(oxa)zol(id)ine class are produced [39]. Nickel(II)-based immobilized metal ion affinity chromatography used to pre-fractionate the metabolome of *S. tropica* CNB-440 and identified DFOA1a, DFOA1b, DFOA2, DFOB, DFOD1, DFOE, DFOD2, DFON compounds, among these DFON was a new siderophore. Based on these studies, the focus on marine actinomycetes is growing for drug discovery. Siderophore metabolome of *S. tropica* CNB-440 was modulated by culture conditions intended to mimic the changeable marine environment. At constant pH and increase in temperature resulted in the increase of DFOA2 and DFOA1 and decreases of DFOB and DFOE, at constant temperature and an increase in pH showed increase in DFOB, DFON, and DFOE decrease in the levels of DFOA2 and DFOA1. DFOB has been used as an iron chelator for iron overload diseases in humans.

Streptomyces olivaceus FXJ 8.012 has isolated from the deep seawater samples of Southwest Indian Ocean reported

to produce two novel oxazole/thiazole siderophores entitled as tetroazolemycins A and B. The structures of these compounds are similar to pyochelin and spoxazomicins. It is difficult to decide the absolute configuration of pyochelin type of siderophore because of their multi chiral centers and isomerization on ring C. So, Liu et al. failed to crystallize the tetroazolemycins A and B, as the structures contain neither hydroxyl groups nor amino acids and CD spectra were not recorded from reference samples [40]. Compounds A and B are screened for heavy metal ion binding ability, results showed that Cu⁺², Zn⁺², and Fe⁺³ have high affinity and Pb⁺², Cr⁺³, and Mn⁺² showed no affinity. Compounds were inactive against *Klebsiella pneumonia* but their Zn⁺² complexes weakly inhibited this pathogen with minimum inhibition concentrations of 125 to 250 µg/ml and 125 µg/ml.

Using LC-HRESI-MS based non-targeted metabolomics, a novel hydroxamate type siderophore fradiamine A and B were isolated from marine actinomycetes *Streptomyces fradiae* MM456M-mF7 from deep-sea sediments of Sagami Bay, Japan. Compounds were purified by Diaion CHP-20P, Sephadex LH-20 column chromatography and eluted with 50% methanol and further purified by HPLC. Fradiamine A, a new siderophore having two alkyl diamines asymmetrically bonded to citric acid core. Fradiamine A and B showed modest antimicrobial activity against *Clostridium difficile* with IC₅₀ values of 32 and 8 µg/ml, respectively. Despite the antibacterial activity, under the presence of Fe⁺³ cancelled dose-dependently [41].

Yang et al. studied the antagonistic activity of *Streptomyces* sp. isolate S073 towards pathogenic *Vibrio parahaemolyticus* using the agar diffusion method. *Streptomyces* sp. S073 produced carboxylate type of siderophore which was confirmed by Vogets test (disappearance of pink colour). The antagonistic activity of S073 was mostly attributed to the siderophore mediated iron competition because most of its life cycle S073 produce siderophores [42]. *Amycolatopsis albispora* WP1T reported to produce a new siderophore, designated as albisporachelin, isolated from samples collected in the Indian Ocean at a water depth of 2945 m. Albisporachelin, have a cyclized hydroxyl ornithine at the C-terminus, at least one N-δ-OH-N-δ-formyl-Orn and includes serine as the only other amino acid residue. The discovery of albisporachelin adds to the diversity of marine-derived siderophores and shows its impact on marine ecology, marine chemistry, and biogeochemistry. Deep-sea derived siderophores are few explored, and this study represented one of the few examples to date [43].

The structures of siderophores from marine actinomycetes are represented in figure 4 and listed in table 1. Yan et al. reported isolation of two novel siderophores Madura statin D1 and D2 which have unusual 4-imidazolidinone cyclic moiety in their structures [44]. To identify the biosynthetic origins of this structure, sequenced the genome of *Actinomadura* sp. WMMA-1423 and found mad biosynthetic gene cluster. The genome sequencing allowed them to propose a hypothesis but needed further studies to clearly understand the biosynthesis of madurastatins.

Transportation of Siderophore-iron in Gram-positive Bacteria

Siderophores entrap traces of iron in the form of very stable complexes, as they are excreted by microorganisms under iron-starvation, and when the complexes have formed, they are taken into the cell by specific cell receptors [45, 46]. Bacteria catch Iron loaded siderophores and transports them into the cytoplasm. As actinomycetes are high G + C Gram-positive bacteria, in this study iron transportation in Gram-positive bacteria is discussed. The cell wall of Gram-positive bacteria has a thick layer of peptidoglycan composed of 40 layers of murein which accounted for 30 to 70% of the dry mass of the wall. This layer consists of teichoic and lipoteichoic acids [47-50]. Siderophores uptake iron complexes using proteins and permeases, which resembles periplasmic binding proteins in Gram-negative bacteria and ATP-binding cassette transporters [51]. The ATP-binding cassette transporter system is a collection of two proteins, where one is used to separate the membrane, acts as a permease, and other is used to hydrolyze, to supply the energy for transportation. As soon as siderophore-Fe⁺³ complex enters the cytoplasm, the Fe⁺³ gets reduced to iron(II) (Ferrous, Fe⁺²) form and Fe⁺² becomes free from the siderophores as shown in figure 5. Once iron got released, the siderophores may get degraded or recycled through the efflux pump system.

Characterization of Siderophores Using Modern Physicochemical Techniques

Intricate tiny compound compositions can be easily analyzed through LC-MS technique. Due to the above-stated application, LC-MS has got importance in different research expenses like medicine and biology like metabolomics, in combinatorial and environmental chemistries for characterization of molecules [52-55]. Many novel iron-holding

proteins namely polypeptide siderophores are also being discovered with the help of LC-MS/MS. In this process, the obtained MS/MS spectrum of newly identified siderophore

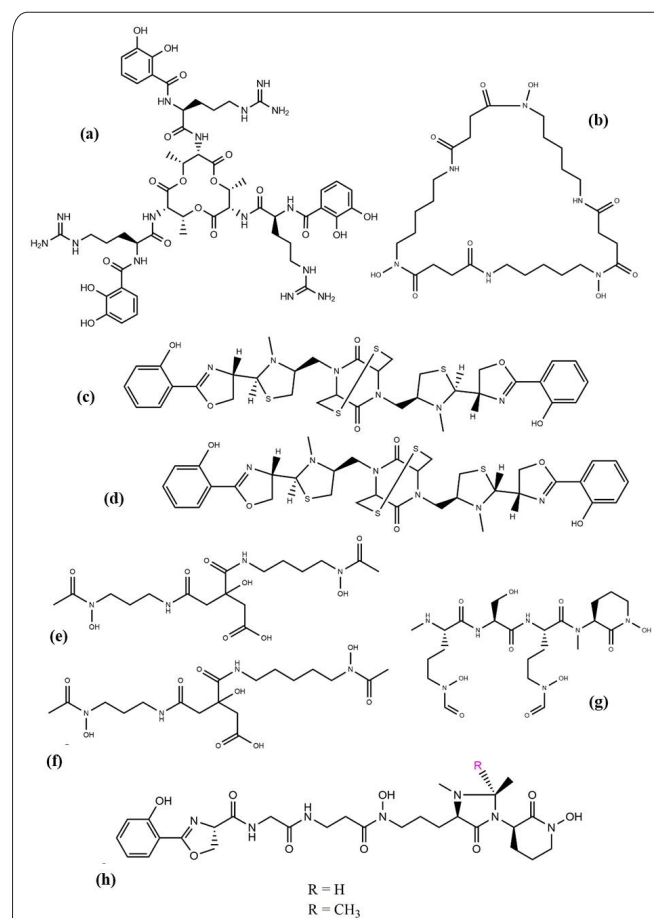
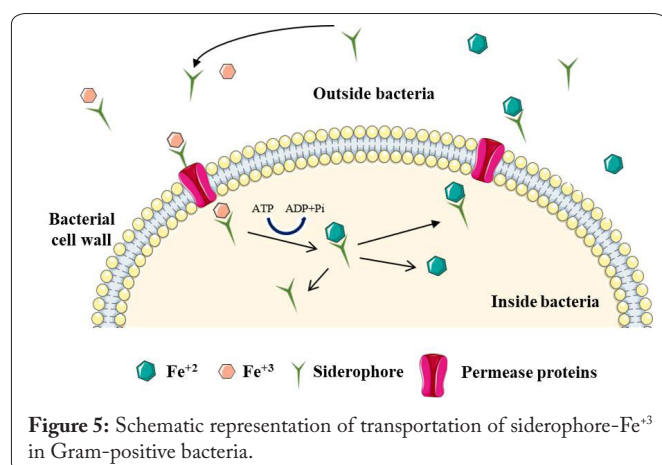


Figure 4: Structures of siderophores from marine Actinomycetes. (a) Streptobactin [36], (b) Nocardamine [38], (c) Tetroazolemycin A [40], (d) Tetroazolemycin B [40], (e) Fradiamine A [41], (f) Fradiamine B [41], (g) Albisporachelin [43], and (h) Madurastatins [44].

Table 1: List of siderophores reported in literature from marine Actinomycetes.

Siderophore	Microorganism	Type	Remarks	Ref.
Madurastatin D1 and D2	<i>Actinomadura</i> sp. WMMA-1423	Phenolate-hydroxamate	Both siderophores contain unusual 4-imidazolidinone cyclic moiety	[44]
Unknown	<i>Streptomyces</i> sp. S073	Carboxylate	Studied excretion of antagonistic substances and impact of siderophore production against pathogenic bacteria	[42]
Albisporachelin	<i>Amycolatopsis albispora</i> WP1	Hydroxamate	Structure of novel siderophore was determined by 1D and 2D NMR and MS-MS experiments	[43]
Fradiamine A	<i>Streptomyces fradiae</i> MM456M-mF7	Hydroxamate	Novel siderophore, showed anti-microbial activity against <i>C. difficile</i>	[41]
Fradiamine B			Sweetness enhancer	
Tetroazolemycin A and B	<i>Streptomyces olivaceus</i> FXJ8.012	Mixed type	Sulfur containing siderophores and binds to several metal ions other than iron	[40]
DFO A1, A2, B, D1, D2, E, and N	<i>Salinispora tropica</i> CNB-440	Hydroxamate	The LC-MS analysis revealed 8 siderophores of DFO class from <i>S. tropica</i> CNB-440. The siderophore metabolome was dynamic and modulated by optimizing micro-environment	[39]
Streptobactin, Dibernarthin, and Tribenarthin	<i>Streptomyces</i> sp. YM5-799	Catecholate	All three siderophores were novel and showed iron chelating activity slightly more than DFO mesylate	[36]
Nocardamine	<i>Citricoccus</i> sp. KMM 3890	Hydroxamate	Novel actinobacteria was isolated and screened for nocardamine and it was showing anti-tumor activity	[38]



is compared with the database which has the data of known siderophores to interpret the characteristics of the new siderophore. The salient feature of LC-MS is the concoction of both the mass-to-charge ratio and retention time. Table 2 summarizes HPLC protocol, which includes columns and methods of marine siderophores. In LC-MS, out of all the soft ionization procedures, ESI is the regularly employed procedure. ESI can develop the mass spectrum of the compound with its minimum amount of fragmentation. It also can assist and mine LC-MS characteristics without disturbing the ions at the molecular level.

Imaqobactin is a siderophore with amphiphilicity extracted from a bacterium (*Variovorax* sp. RKJM285) isolated from the Arctic region. In this study, the core-shell 100 Å C18 column of Phenomenex was used for accomplishing chromatography. The injection volume was 10 µl and the flow rate for the entire process was maintained at 500 µl/min. Two mobile phases were used in this process, one was 0.1% formic acid with water which acts as solvent A, and the other was 0.1% formic acid with ACN which acts as solvent B. A gradient of these two solvents ranging from 95% of solvent A, 5% of solvent B to 100% solvent B for 4.8 min trailed by a 3.2 min hold with the above-mentioned flow rate and injection volume. UV 200 to 600 nm, ELSD, and ESI-MS were the detectors used. Sample analysis of LC-HRMS revealed the two ions which are eluting at the same time. One of them has m/z ratio of 934.5038 $[M + H]^+$ and the other has 987.4168 $[M + H]^+$, based on these ratios their suggested molecular formulas are $C_{41}H_{71}N_7O_{17}$ and $C_{41}H_{68}FeN_7O_{17}$, respectively. The first one, $C_{41}H_{71}N_7O_{17}$ has 53 units less m/z ratio when compared to $C_{41}H_{68}FeN_7O_{17}$. This loss of mass might be related to the Fe^{+3} loss, which is typical for siderophores that bind iron [60].

Characterizing structures of compounds using MS/MS is a challenging task due to the complex melange of tiny molecular structures [66]. A marine bacterium namely *Shewanella woodyi* MS32 produced a set of novel siderophores (Woodybactins A, B, C, and D) with fatty acyl group. Waters Xevo G2-XS QT of MS was used to determine the molecular multitudes. This instrument possesses waters BEH C18 column and positive mode ESI attached to an ACQUITY UPLC-H-Class system. Mobile phase used was ACN with 0.1% formic acid in double-distilled water with 0.1% formic acid and a gradient of 0 to 100% was applied linearly. The woodybactins

(A, D) molecular ion peaks of m/z ratio were determined as 463 and 491, respectively, whereas both woodybactins B and C had peaks 477. Peculiarly, the difference in mass between woodybactins A and B is the same as woodybactins C and D which is 14 units. This indicates the difference between CH_2 groups. The available data suggests that the fatty acid chains of woodybactins A to D might most probably vary in length [56].

For identification of an unknown compound and to identify its structural aspects, MS/MS is the most suitable technique. The m/z ratio of selected siderophores and type of ionization are listed in table 3. In 2005, Owen et al. [23], identified a set of siderophores with amphiphilicity from *Marinobacter* sp. strain DS40M6 and strain DS40M8 and named them marinobactins A to E. For these marinobactins, the head group is made of protein, which manages the fatty acid chain and Fe^{+3} . A few years later in 2007, Martinez and Butler, identified another marinobactin with C18 fatty acid and having a single double bond, namely marinobactin F. The hydrophilicity of marinobactin F is much higher than the other A to E marinobactins. All these marinobactins are established with the help of electrospray mass spectrometry and HPLC (analytical). A VG-Fisons platform II (Micromass) with quadrupole MS was used which was coupled with MichromBioResources HPLC unit, for injecting directly. For marinobactins A to E the source temperature and a cone voltage are 70 °C and 65 V, respectively, whereas for marinobactin F the source temperature and a cone voltage are 90 °C and 80 V, respectively, are enough for fragmenting. The marinobactin F molecular ion peaks of m/z ratio were determined as 1014 $(M + H)^+$ [21]. In 2000, Martinez et al. identified two new members of the aquachelins family, namely aquachelins J and I, which were identified from *Vibrio* sp. HC0601C5 and *Halomonas meridiana* strain HC4321C1 with the help of reverse phase HPLC. The ESI-MS and tandem mass spectrometry were executed on Micromass Q-TOF2 with collision gas as Argon to determine the structural aspects of the above mentioned aquachelins [69].

To identify the siderophores in marine water, the samples were pre-treated with solid-phase extraction and coupled with LC-tandem MS. ZORBAX SB-C18 reversed phase column (50 mm x 2.1 mm, 1.8 µm, Agilent, USA) was used to separate the sample using formic acid 0.1% (v/v) and methanol as mobile phase A and B at a flow rate of 0.25 ml/min. The MS was performed under multiple reaction monitoring and ESI-positive mode. This method is used in analyzing siderophores under HNLC regions and exhibited advantages such as high enrichment factor, matrix effect, in accurate quantification of ability and good recovery [75].

MALDI-TOF-MS is a rapid and economical technique used to identify several biomolecules and bacteria based on ribosomal MS data. Successive developments in the instrumentation resulted in better-resolved spectra of perfectly folded proteins. Total acquisition and analysis of intact proteins and rare metabolites of 384 bacterial colonies can be completed in less than four hours by using MALDI-TOF-MS but it requires basic expertise for sample preparation and to operate in comparison with regular instrumentation like Orbitrap, qua-

Table 2: HPLC column and method reported in literature for marine siderophores.

Siderophore(s)	Instrument	Column	Method			Ref.
			Gradient system	Mobile phase	Flow rate	
Woodybactin	HPLC	YMC 20 x 250mm C18-AQ column	5% to 100% methanol	Methanol, Water	-	[56]
Myxochelin B	LC/MS	Nucleodur 100-5 C18 ec VarioPrep column (125 x 21 mm, 5 µm; Macherey-Nagel)	37% to 53% methanol over 63 min, 63% to 100% over 2 min, and 100% methanol for 7 min	Methanol, Water	4 ml/min	[57]
Massiliachelin	RP-HPLC	Nucleodur 18 PAH column (250 x 8.0 mm, 3 µm, Macherey Nagel)	10% methanol for 5 min, from 10% to 100% over 35 min, 100% for 10 min, followed by 10% for 10 min	Methanol, Water	-	[58]
Pacifibactin	RP-HPLC	YMC 20 x 250 mm C18-AQ column	10% methanol in water to 30% methanol in water 10/90% water/methanol over 40 min	Methanol, Water	-	[59]
Imaqobactin	LC-HRMS	C18 column (Phenomenex, Kinetex, 1.7 µm 50 x 2.1 mm)	95% water/0.1% formic acid and 5% ACN/0.1% formic acid over 4.8 min	ACN, Formic acid	500 µl/min	[60]
Albisporachelin	HPLC-MS	C18 column (Waters Xbridge, 4.6 mm x 50 mm)	5 to 25% ACN in water (each with 0.05% TFA) over 60 min	ACN, Water	1 ml/min	[42]
Fradiamines A and B	HRESI-MS	SPELCO Ascentis Express C18 column (2.1 mm ID x 50 mm)	95% A to 0% A (5 min), 0% A (5 to 8.5 min), 95% A (8.5 to 12 min); 0.1% formic acid aq. (A) and 0.1% formic acid-ACN (B)	Formic acid, Formic acid-ACN	0.4 ml/min	[41]
Pseudoachelin A	LC-MS/MS	Reverse phase C18	0 to 100% Methanol	Methanol	2 ml/min	[61]
Thalassosamide	LC-MS	Phenomenex Luna C18 reversed-phase column (250 x 4.6 mm, 5 µm)	10 to 40% CAN-water with water containing 0.1% acetic acid over 25 min, 4.0 mg/ml	ACN-Water, Acetic acid	1.0 ml/min	[62]
Variochelins	LC-MS	C18 column (Betasil C18, 150 x 2.1 mm, 3 µm; Thermo Scientific)	Methanol-water gradient from 50% to 100% over 20 min	Methanol, Water	0.2 ml/min	[63]
Avaroferrin	LC-MS	C18 Inertsil ODS-3, 2 x 100 mm	20% to 60% Methanol	Methanol	0.2 ml/min	[64]
Moanachelins	RP-HPLC	C4 column (250 mm length x 20 mm diameter, Higgins)	100 % A (0.05 % TFA in water) to 100 % B (0.05 % TFA in 80 % methanol, 20 % water) over 37 min	Methanol, Water	-	[65]
Tetroazolemycin A	HPLC	Waters Xbridge ODS (10 x 150 mm, 5 µm) column	Methanol:water = 70:30, v/v	Methanol	-	[40]
Ochrobactin	RP-HPLC	Preparative C4 column (250 mm x 20 mm Higgins)	50% A (0.05% TFA in water), 100% B (0.05%TFA in 80% Methanol, 20% water) over 15min	Methanol, Water	-	[66]
Nocardamine	HPLC	C-18 column 10.0 mm x 250 mm, 5 µm, Supelco	(30 to 60%) of Methanol:water over 25 min	52% Methanol or in 27% ACN	2 ml/min	[38]
Aquachelin	RP-HPLC	C4 column (250 mm length x 20 mm diameter)	50% A [0.05% TFA in water] to 100% B (0.05% TFA in 80% Methanol) over 15 min	Methanol, Water	-	[28]
Streptobactin	RP-HPLC	TSK gel ODS 80Ts, ϕ2.0 x 25 cm	20% to 50% aqueous ACN containing 0.1% TFA in 30 min	ACN	10 ml/min	[36]
Loihichelins	RP-HPLC	C4 column (250 mm length x 22 mm diameter)	80% A (0.05% TFA) and 20% B (0.05% TFA) in 19.95% water and 80% ACN over 45 min	ACN, Water	-	[29]
Marinobactin	HPLC	C4 reversed-phase column (Vydac, 5 mm ID x 250 mm length)	100/0 (% A/B) for 7 min to 0/100 over 25 min; and a hold at 0/100 for 3 min [A = 99.95% water and 0.05% TFA; B = 19.95% water, 0.05% TFA, and 80% ACN]	ACN, Water	-	[21]
Synechobactin A to C	HPLC	C18 reversed-phase column (Vydac 10 mm ID 3 250 mm length)	20% to 50% ACN with 0.05% TFA	ACN	100 ml/min	[67]
Petrobactin sulfonate	RP-HPLC	(Vydac C4 column (10 mm, 22 mm ID x 250 mm)	ACN/water gradient (0% to 60%) over 35 min	ACN, Water	-	[32]
Amphibactin	HPLC	C4 reversed-phase column (Vydac)	100/0 (% A/B) to 0/100 (% A/B) over 37 min; A = 99.95% water and 0.05% TFA; B = 19.95% water, 0.05% TFA, and 80% Methanol	Methanol, Water	-	[22]
DFO G	HPLC	C18 or C4 reversed phase column (Vydac 10 mm ID 3 250 mm length)	100/0 (% A/B) to 0/100 over 35 min; A = 99.95% water and 0.05% TFA; B = 39.95% water, 0.05% TFA, and 60% Methanol	Methanol, Water	-	[68]

Table 3: Showing MS data reported in literature for marine siderophores.

Instrument	Ionization	m/z ratio	Mode	Compounds	Ref.
HR-ESI-MS	ESI	513.3655 (M + H) ⁺	-	Fw0622	[70]
HR-ESI-MS	ESI	467.2033 (M + H) ⁺	-	Massiliachelin	[58]
HR-ESI-MS (Q-TOF)	ESI	372.1919 to 408.1747	Positive	Myxochelin B (1 to 9)	[57]
HR-ESI-MS (Q-TOF)	ESI	370.1759 to 390.1647	Positive	Pseudochelin A (4 to 9)	[57]
HR-ESI-MS	ESI	923.4081 (M + H) ⁺	Positive	Pacifibactin	[59]
HR-ESI-MS (Q-TOF)	ESI	463, 477, 477, and 491	positive	Woodybactins A to D	[56]
HR-ESI-MS	ESI	560.2712 (M - H) ⁻	Negative	Albisporachelin	[42]
LC-HR-MS, MS/MS	ESI	934.5038 (M + H) ⁺	-	Imaqobactin	[60]
FTICR-MS	ESI	895.3995	Negative	Amphibactin Ua	[71]
FTICR-MS	ESI	897.4151	Negative	Amphibactin Va	[71]
LC-HR-ESI-MS	ESI	435.2086 and 449.2242 (M + H) ⁺	Positive	Fradiamine A and B	[41]
HR-ESI-MS (MALDI-TOF/TOF)	ESI	1074.604 (M + H) ⁺	-	Variochelin A	[63]
LC-MS-8040	ESI	419, 405, 401, 391, 387, and 373	-	Avaroferrin	[64]
HR-ESI-MS	ESI	757.1971 and 757.1965 (M + H) ⁺	-	Tetrozolemycins A and B	[40]
HR-ESI-MS (Q-TOF II)	ESI	778, 788, 800, 802, 816, and 828 (M + H) ⁺	-	Moanachelins	[65]
LC-MS	-	628.29 (M + H) ⁺	-	DFO N	[39]
ESI-MS (Q-TOF2)	ESI	793, 821, and 849	-	Ochrobactin-OH A to C	[66]
HR-ESI-MS (Q-TOF)	ESI	5909.3407 (M - H) ⁻	-	Nocardamine	[38]
ESI-MS (Q-TOF2)	ESI	830.54 (M + H) ⁺	-	Amphibactin S	[28]
ESI-MS (Q-TOF2)	ESI	804.55 (M + H) ⁺	-	Amphibactin T	[28]
HR-FAB-MS	ESI	1180.5004	-	Streptobactin	[36]
GC-MS	ESI	930, 974, 956, 958, 984, and 986	-	Loihichelins A to F	[29]
LC-MS	-	1014 (M + H) ⁺	-	Marinobactin F	[21]
HR-ESI-MS (Q-TOF)	ESI	614.261, 586.23, and 558.198	-	Synechobactins A to C	[67]
HR-ESI-MS	ESI	799.3199 (M + H) ⁺	Negative	Petrobactin sulfonate	[32]
ESI-MS	-	1078.4 and 1106.5 (M + H) ⁺	-	Pseudoalterobactin A and B	[33]
ESI-MS	ESI	719.3614 (M + H) ⁺	Positive	Petrobactin	[31]
ESI-MS	ESI	619.3647 (M + H) ⁺	-	DFO G	[68]
FAB-CI-MS	CI	373.21 (M + H) ⁺	-	Putrebactin	[72]
VG ZAB-E FAB-MS	-	349.0944 (M + H) ⁺	-	Anguibactin	[73]
SI-MS	SI	401 (M + H) ⁺	-	Bisucaberin	[74]

druple TOF, and FT-ICR mass spectrometers [76].

Variovorax boronicumulans produces variochelins, lipopeptide siderophores differ in biosynthesis when compared with most of the other lipopeptide siderophores where polyketide synthase is involved. The head group of variochelin A and connectivity of constituents were analyzed by tandem MS. The three bidentate ligand groups include two hydroxamate functions and hydroxy carboxylate (i.e., the β-hydroxyaspartate residue) were identified by MALDI-TOF/TOF (Bruker Ultraflex spectrometer) fragmentation [63]. The DFO-E is an ideal siderophore used for iron chelation therapy, isolated from *Streptomyces* bacteria. It requires cost effective industrial production for *in vitro* and animal studies. Approximately, 97% of pure DFO-E was analyzed by two-step purification process using HPLC. MALDI-TOF-MS analysis demonstrated the purified DFO E always contains traces of DFO D2 [77]. Guerrero-garzón et al. isolated ten strains of *Streptomyces* from marine environment for secondary metabolites Biosynthetic gene cluster analysis. LC-MS analysis of strain ADI96-02, led

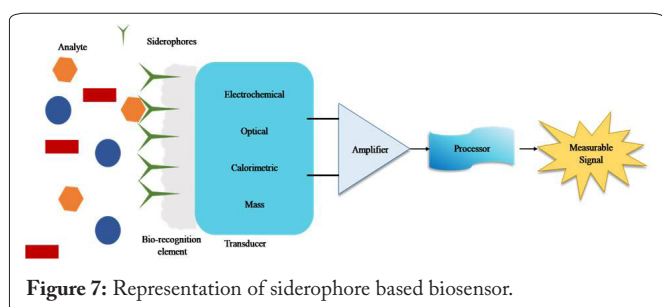
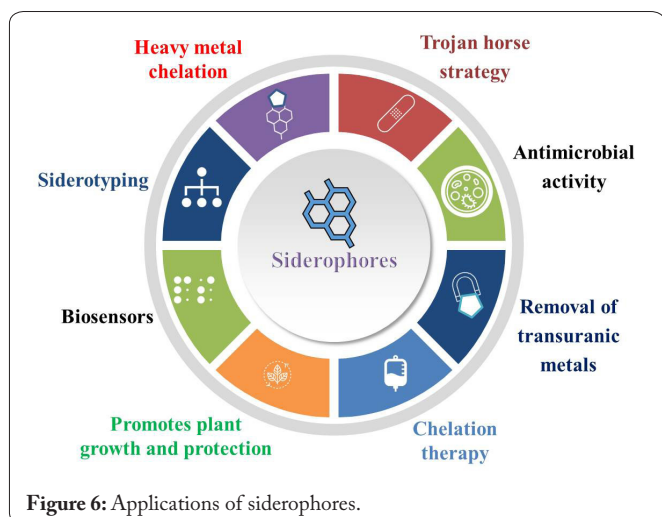
to detection of several different metabolites. Among them one of the main compound identified as nocardamine (DFO E) [78].

Applications of Siderophores

Siderophores, small and unique biological organic molecules produced under iron-limited conditions by microorganisms, has insightful applications in the following topics (Figure 6).

Biosensors

Recently, siderophores were used as biosensing platforms to detect metal ions because of their high selectivity and sensitivity, cost-effectiveness, the suitability of handling, rapid response, and non-toxicity [79]. Biosensor is an analytical device capable of generating specific quantitative and semi-quantitative information using a biomolecule coupled to an electrical device (transducer), an amplifier to enhance the signal to noise



ratio [80-82]. Siderophores have high affinity and specificity towards numerous metals and their receptors supply the basis for using them as sensors or probes [83].

Currently, some siderophores based biosensors and nano-sensors have initiated with substantial success for different metal ions detection such as copper [84], iron [85-89], aluminum [90, 91], and molybdate [92-94]. Several siderophore based techniques developed to detect and estimate metal ions, especially iron. Among them, fluorescent siderophores were considered as highly sensitive, because they are capable to detect low concentrations of analyte and shows rapid response rates. Biosensors utilize various electrochemical properties of siderophores to detect metals. Figure 7 represents the schematic diagram of siderophore based biosensor.

Fluorephore molecules are developed by using fluorescence siderophores which are dynamic receptors for iron ions detection [95]. The PVDs are natural fluorescent siderophores mostly used for the detection of iron. These molecules are yellow green, fluorescent siderophores which are produced by *Pseudomonas fluorescenes*, *P. aeruginosa* and other fluorescent *Pseudomonads* [96]. The hydroxamate and catecholate groups of PVDs reacts with iron and form hexa-coordinate complexes, because of their high stability constants (10^{22} to $10^{32} M^{-1}$) it protects against hydrolysis and enzymatic degradation [97]. Azobactin is another PVD type siderophore produced by nitrogen fixing soil bacteria *Azobacter vinelandii*. The selective sensors were identified iron in tap water and human serum (FI system) successfully [98, 99].

In recent times, several studies have been reported on the usage of siderophores in microbial pathogen detection. It de-

pends on the high affinity of siderophores towards cell surface receptors of bacteria, which identifies and facilitates the siderophore-iron complex and immobilization of siderophores. Doorneweerd et al. introduced the method to detect siderophore based siderophore detection by immobilizing PVD on gold-plated glass chips to identify the pathogen like *P. aeruginosa*. A treated polydimethylsiloxane stamp with PVD-Bovine serum albumin conjugate was used as pattern for gold-plated glass surface. This technique is significantly faster than polymerase chain reaction for pathogen detection because it takes only fifteen minutes for maximum binding of *P. aeruginosa* to PVD [100].

The biosensors were designed to detect pathogens by developing new methodologies, discovering siderophore binding proteins from pathogen cell extracts. Petrobactin is a biscatecholate, α -hydroxy acid siderophore isolated from marine bacteria and other human pathogens *Bacillus anthracis*, *B. subtilis*, and *B. cereus* [101, 102]. Siderophore-based piezoelectric biosensor was developed by Inomata research group for the detection of several microorganisms using gold NPs [103-105]. They considered as mass measurement devices that depend on detecting the change of resonance frequency on a Quartz Crystal Microbalance, this change proportional to the mass binding to the electrode [83].

Siderotyping

Siderotyping or siderophore typing is a method to characterize the microbes based on the type of siderophores they produce [45, 106]. It can be done in both analytical and biological method. In the analytical method, the physicochemical properties of siderophores were studied using HPLC-MS and in biological method, using molecular biology techniques like immunoblot detection directly measure the siderophore mediated iron in microbial cells [107]. In siderotyping, major classification is based on siderophore producers' group and non-siderophore producers' group.

About 400 strains of fluorescent and non-fluorescent *Pseudomonas* sp. are investigated and depending on siderophore type they classified into 28 taxa and using MS analysis, 68 fluorescent *Pseudomonas* were identified by studying their PVDs [107-109]. Siderotyping can also be used as a chemotaxonomic marker to identify other types of bacteria for example *Mycobacterium* sp. and *Burkholderia* sp. depending on the difference in chemical structures of mycobactin and ornibactins, respectively [110, 111].

Improves the growth of uncultivable bacteria

Kaerberlein et al. reported that siderophores can be acts as a growth factor to promote the growth of uncultivable microorganisms by co-culture of microorganisms [112, 113]. Certain siderophores produced by actinobacteria can mediate actinomycete interactions. The Inter specific stimulatory events mediated by putative diffusible metabolites for the antibiotic production and morphological differentiation from *Streptomyces* sp. occur at a high rate. *Streptomyces griseus* produces DFO E that shows identical stimulatory effects on the growth and development of *S. tanashiensis*. Ferrichrome and nocobac-

tin produced by microorganisms doesn't show any impact on the growth of uncultivable microbes (Figure 8). But DFO E promotes secondary metabolites production and morphological differentiation in several actinomycetes strain [114]. The siderophore genes of amycolin produced by *Amycolatopsis* sp. A4 was downregulated when they grow nearby *S. coelicolor* because it inhibits the aerial hyphae formation (development arrest). But *Amycolatopsis* sp. AA4 utilizes DFO E produced by *S. coelicolor* [115]. Therefore, the species specific siderophores can modify the morphological differentiation and patterns of gene expression in actinomycetes interactions and several uncultivable organisms can be cultivated and purified as pure culture. The pure cultures of uncultivable microorganisms can be investigated for potential applications in various fields [24].

Medicine

Trojan horse strategy

The efficacy of therapy can be improved by developing various promising drug delivery methods [116]. For delivering drug molecules of less size Trojan horse therapy is the most promising one. This therapy works by transporting drug molecules through membranes, which act as barriers and thereby enhancing the in-take of drug molecules by cells. The practical application of this method has failed *in vivo* due to its toxic side-effects. These effects are due to the unregulated transport of drug molecules into the cells [116].

The Trojan horse strategy can be applied to antibody conjugated siderophores called sideromycins. The intake of drugs will be efficient and easy as the cells take up iron part of sideromycins through the cell gates and along with iron they also carry the conjugated antibiotic into the cell. In most of the bacteria, the outer membrane is very selectively permeable; by applying this strategy the permeability issue of drug molecule can be resolved with ease. The main parts of drug-siderophore conjoint are three and they are linker, siderophore and the drug (Figure 9). The key role players in this conjoint are siderophore and drug molecule, siderophore has to bind the iron whereas drug has the antibacterial activity when it is released from the complex. The role of the linker is not only to connect the drug molecule and siderophore but also to regulate the drug release from the siderophore-drug molecule conjoint [47, 117-119].

When this conjoint reach the bacterial cytoplasm with the help of a siderophore, it slowly releases the drug which starts microbial extermination. This action of the conjoint can trigger an equal and opposite reaction which blocks the further transport of iron into the cell [120]. This strategy of Trojan horse not only employs iron but also employs other heavy metals like gallium, which can disturb the microbial metabolism of iron and inhibits the formation of biofilm [121]. Following are few examples of drug-siderophore conjoint, carbacephalosporin-biscatecholate-monohydroxamate siderophore, ampicillin-triscatecholate siderophore, ciprofloxacin-trihydroxamate siderophore, vancomycin-catecholate-hydroxamate siderophore and amoxicillin-triscatecholate siderophore [122-124]. Extensive research is being carried out to synthesize man-made siderophores and to complex them with effective antibiotics for treating multi-drug resistant microbial infections and for

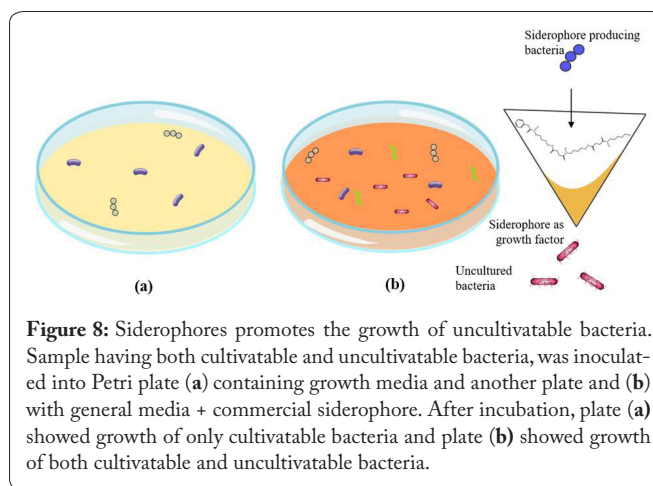


Figure 8: Siderophores promotes the growth of uncultivable bacteria. Sample having both cultivatable and uncultivable bacteria, was inoculated into Petri plate (a) containing growth media and another plate and (b) with general media + commercial siderophore. After incubation, plate (a) showed growth of only cultivatable bacteria and plate (b) showed growth of both cultivatable and uncultivable bacteria.

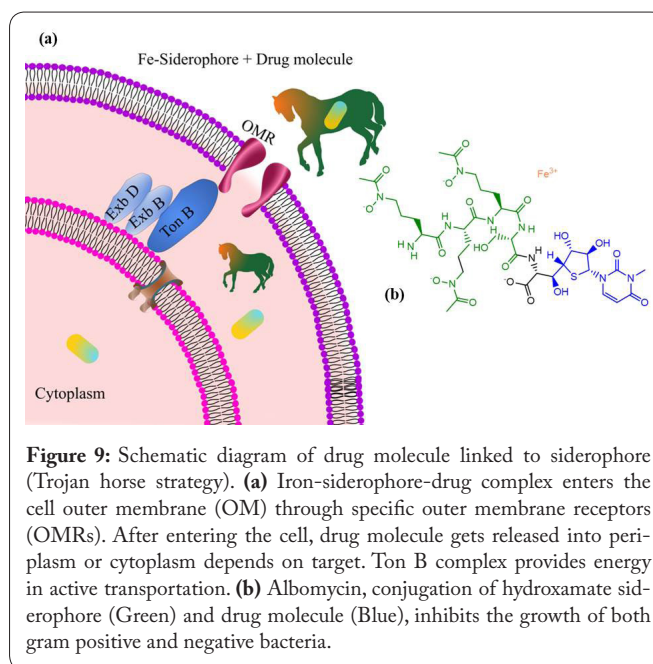
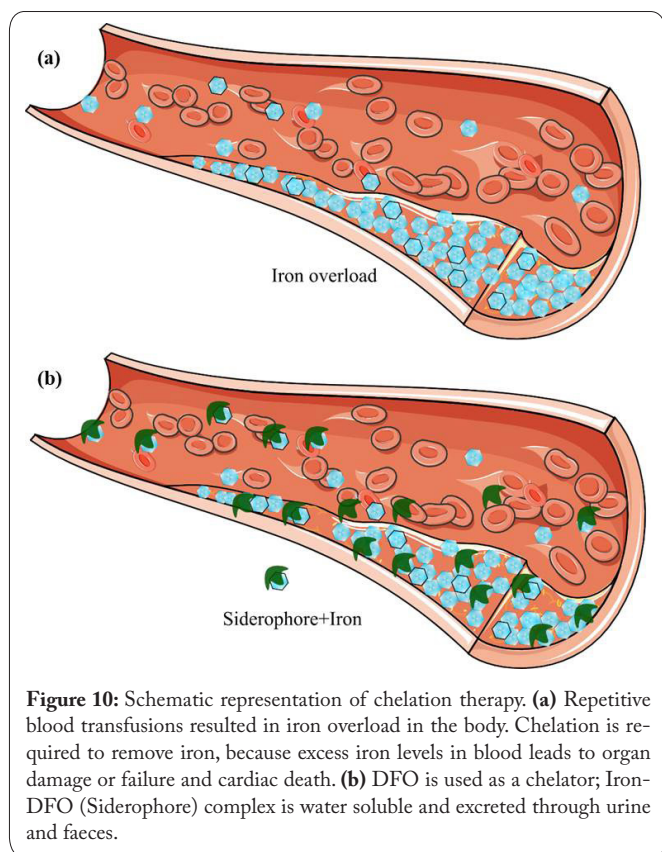


Figure 9: Schematic diagram of drug molecule linked to siderophore (Trojan horse strategy). (a) Iron-siderophore-drug complex enters the cell outer membrane (OM) through specific outer membrane receptors (OMRs). After entering the cell, drug molecule gets released into periplasm or cytoplasm depends on target. Ton B complex provides energy in active transportation. (b) Albomycin, conjugation of hydroxamate siderophore (Green) and drug molecule (Blue), inhibits the growth of both gram positive and negative bacteria.

treating many other diseases in humans [8, 49, 125].

Iron overload therapy

There are a few diseases which are caused due to the overload of iron and siderophores have the potential to be used as a treatment for those. For treating disorders like sickle cell anaemia, beta-thalassemia, blood transfusion is a must [126]. The red blood cells reach their graveyard, spleen at the end of their life span and die. This is the only mechanism of iron removal in the human body and no other mechanism exists. Consecutive blood transfusions result in an elevated level of iron in the body which is very harmful to the vital body parts and especially the liver. So this iron overload should be minimized to reduce the risk of damaging vitals. Siderophore associated drugs have the potential to minimize iron overload in the body and can be used in treating many disorders [127]. One such siderophore associated drug is Desferal [128]. It contains DFO mesylate, which is an iron chelating siderophore, primarily used for treating disorders like sickle cell anaemia and thalassemia major [129-131]. The diagrammatic representation of chelation therapy is shown in figure 10.



Antimicrobial activity

Nowadays, multi-drug resistant microbes are evolving very rapidly, and the old antibiotics have significantly reduced showing effect towards them. For this reason, researchers have started exploring new horizons for effectively handling this issue and came up with many discoveries and one among them is usage of siderophores [34].

To stay alive, few parasites require an iron source and *P. falciparum*, *Leishmania* sp., and *Trypanosoma cruzi* are some among them. For most of the parasites, life cycle begins in insects and later, they infect mammals for completing their life cycle, in the parasite's life cycle (especially in mammals) they depend on iron taken in by the hosts [132]. Lytton et al. experimented and reported a curative effect on parasites in mice. A Swiss mouse was administered 370 mg/kg hydrophobic chelator of iron dose in combination with coconut oil subcutaneously 3 to 4 times with a time interval of 8 h. The results were surprising with two-to-three-fold decreases in parasite concentration in its body and the infected mice had an increased survival time [133]. According to Loyevsky et al. DFO B is a potent drug used for malaria disease and action of it might be based on its ability to chelate iron lying in the cytoplasm of plasmodium parasite. The anti-malarial effect of DFO B has been proved in both *in vitro* and *in vivo* studies but the drawback is its limited time of action. Despite continuous exposure of drug, the suppression of parasite is too slow to develop the anti-malarial activity [134].

According to Pradines et al. DFO has very less absorption into the blood when administered orally and even if adminis-

tered as intravenous it has a very short half-life [135]. *Crassostrea virginica*, an oyster amasses large amounts of iron in its body leading to more parasitic attacks and easy proliferation of parasites like *Perkinsus marinus*. The DFO works effectively for *C. virginica* when given in a proper continuous dosage [136].

Removal of transuranic elements

With depleting energy reserves scientists are working on new reliable technologies for energy generation to meet day to day increasing human needs and one such technology is the generation of electricity through nuclear energy. This has paved a way for the increase of vanadium, aluminum, etc., which are transuranic elements [8]. The increasing levels of these transuranic elements are not good for life in any form. Apart from the environmental issues, patients who undergo dialysis for a very long period accumulate aluminum in brain, which is called encephalopathy due to dialysis. Aluminum overload is also observed in patients with end-stage renal failure. To treat these aluminum overload related disorders siderophores like desferal are being employed [8]. Desferol forms aluminoxamine complex in the presence of aluminum (Figure 11). This complex is easily dissolved in water and gets excreted along with faeces and urine [8, 137-140]. It's been already reported that desferal has the potential to reduce the amount of vanadium from the body. According to Nagoba and Vedpathak, it's been reported that usage of Desferal removes vanadium by 25% in lungs, 26% in liver, and 20% in kidneys [8].

Cancer therapy

Cancerous cells divide unrestingly to form tumours. For this uninterrupted cell division, continuous growth and development, these cells must have high concentrations of iron. So, cancerous cells require more iron than the normal non-cancerous cells. The relationship between cancer development and iron overload has been under continuous review ever since the fact of their dependency has been established [141]. According to Nakouti et al. siderophores, especially iron chelators are being employed as they are restricting the growth of cancer cells. For instance, patients suffering from neuroblastoma were administered with DFOs and there was a significant reduction in development of belligerent cancer cells [142]. Out of the available DFOs, DFO E has been reported to have cytotoxicity effect through induced apoptosis towards malignant melanoma cancers [1].

Toxic and heavy metal bioremediation

Though heavy metals (Pb, Cd, Hg, Cu, Cr, Fe, Zn, Al, Co, Mn, and Ar) are present naturally in soil and water. Due to rapid industrialization and other activates like mining, usage of pesticides and fertilizers, the concentration of heavy metals increased and disposal of these metals without treatment poses a persistent risk to human health and environment. The bioremediation of heavy metals became a challenging task because these metals cannot be degraded completely but can transform from one organic complex to another (Figure 12) [34, 128]. Presently, the investigation on the usage of siderophores for bioremediation potentially increased. Neubauer et al. reported that DFO B, a siderophore can chelate Co^{+3} at high pH con-

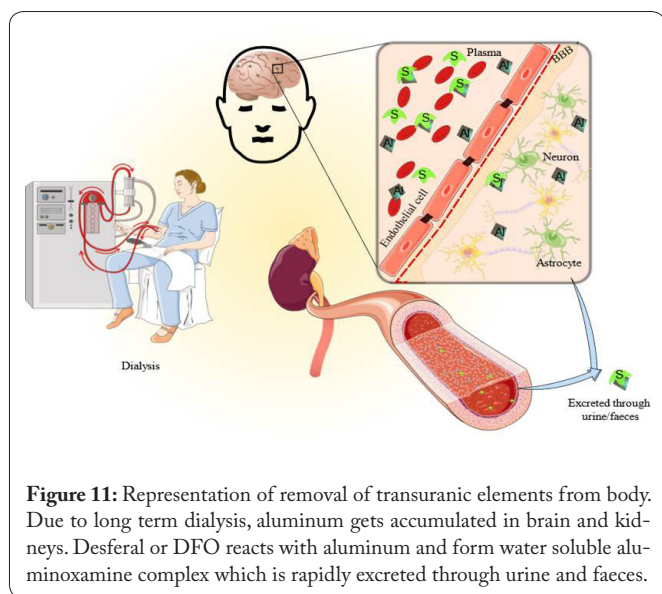


Figure 11: Representation of removal of transuranic elements from body. Due to long term dialysis, aluminum gets accumulated in brain and kidneys. Desferal or DFO reacts with aluminum and form water soluble aluminohydroxamate complex which is rapidly excreted through urine and faeces.

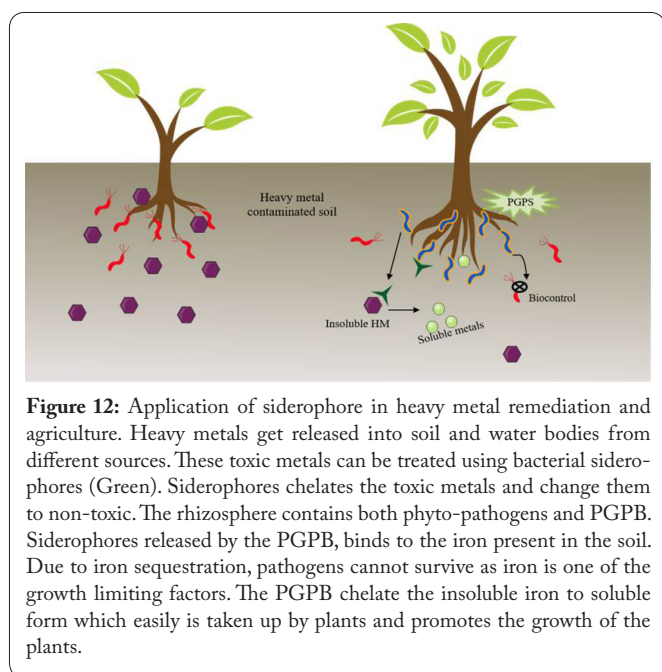


Figure 12: Application of siderophore in heavy metal remediation and agriculture. Heavy metals get released into soil and water bodies from different sources. These toxic metals can be treated using bacterial siderophores (Green). Siderophores chelates the toxic metals and change them to non-toxic. The rhizosphere contains both phyto-pathogens and PGPB. Siderophores released by the PGPB, binds to the iron present in the soil. Due to iron sequestration, pathogens cannot survive as iron is one of the growth limiting factors. The PGPB chelate the insoluble iron to soluble form which easily is taken up by plants and promotes the growth of the plants.

ditions than Fe^{+3} [143]. Azotobactin and azotochelin siderophores produced from *A. vinelandii* used for the acquisition of Mo and V [98].

Raoultella sp. strain X13 Cd resistant microbe absorbs Cd that present in the soil by ion exchange and chelation enhances the production of indole acetic acid and siderophores for plant growth. The siderophores produced by strain X13 reduces the bioavailability of Cd in Cd stressed soils [144]. Some siderophores isolated from actinobacteria reduces the Cd uptake by bacteria. Under Ni contamination, *S. acidiscabies* E13 secreted hydroxamate type of siderophores. It promoted the growth of cowpea by binding Ni and Fe, inhibited uptake of Ni and supplied Fe for the plant growth [145]. *P. azotoformans* produced the mixed type of siderophore (catechol and hydroxamate) showed a high affinity towards several metals Cd, Pb, Ni, Ar, Al, Mg, Zn, Cu, Co, and Sn other than Fe. Among them, Ar removed 92.8% by five washes using siderophore and 77.3% by

EDTA, 70.0% by citric acid [146].

Vibrio parahaemolyticus, marine estuarine entero-pathogen reported to produce vibrioferrin a citrate-based siderophore that shows less affinity towards iron but observed as borate complex, though borate was not added to isolating media. Authors proposed that siderophore forming a complex with boron from borosilicate glassware used during experimentation [147-149]. Shinozaki et al. reported that *Pandora* sp. HCo-4B produced thermostable siderophore chelated Co^{+2} , when organism grown in Co^{+2} supplemented medium. The siderophore binds to Co^{+2} in 1:1 ratio, it gets absorbed to C18 column and eluted with ethanol [150].

In the marine environment, petroleum hydrocarbons are one of the major problems. For the bioremediation of petroleum hydrocarbons in marine ecosystems, microorganisms play a significant role [151]. Under iron starvation, the marine microbes produce siderophores, by facilitating the iron acquisition the siderophore participate in the degradation of petroleum hydrocarbons [31]. *M. hydrocarbonoclasticus* oil-degrading micro bacterium secreted petrobactin siderophore and structurally characterized. *M. Hydrocarbonoclasticus* reported to produce another sulfonated siderophore called petrobactin sulfonate, catechol type [32]. Gauglitz et al. reported that amphiphilic siderophores called ochrobactins were produced from marine bacterium *Vibrio* sp. that isolated from the Gulf of Mexico after the Deepwater Horizon oil spill in 2010. Ochrobactins, may contribute to the degradation of petroleum hydrocarbons [66].

Agriculture

Promotes plant growth

The PGPB are a different set of bacteria which aren't harmful and can increase the tolerance to stresses, growth rate, and resistance towards diseases in plants. They are wide range of bacteria and exist in different habitats like soil especially the phyllosphere and rhizosphere of plants. Some bacteria exist as symbionts and especially as endophytes that live in the interior tissues of plants [145, 152-154]. According to Omidvari et al. at neutral pH the level of available iron required for microbial growth is 0.006 to 0.01 mmol/ml, whereas plants require more concentration of iron than microbes i.e., 0.010 to 0.017 mmol/ml [155]. The fact that PVD siderophores produced by various *Pseudomonas* species can boost the growth of plants is proved beyond doubt [156, 157]. So, all these bacteria which boost the plant growth are referred to as PGPB [158]. In 2000, Masalha et al. [159], experimented on plants to know the importance of microbes in the plants iron takes up. For this, plants were grown on soil with loess loam texture and care was taken to maintain asepsis in the soil for one plant and microbes were allowed to grow in another. After some time, it was observed that plant roots in soil with microbial growth were observed to have more iron than the plant roots with aseptic soil.

On the other hand, the plants are grown on aseptic soil were observed to have iron malnutrition and even didn't have a proper vegetative growth. They have concluded that the siderophores produced by soil microbes can be an effective iron source for plants [159]. According to Rungin et al. *Strepto-*

myces sp., an endophytic bacterium in Thai jasmine rice plant enhanced the roots and shoots remarkably [160]. In 2013, Qi and Zhao have reported enhanced salt stress tolerance in cucumber by siderophore produced by *Trichoderma asperellum* [161]. Apart from siderophores of microbial origin, there are some siderophores which are produced by the plant itself. They are called phyto-siderophore, whose working is similar to microbial siderophores. When an iron malnutrition plant was supplemented with phyto-siderophore, plant showed better growth and the symptoms related to iron shortage were significantly reduced. For enhanced iron uptake of plant and its growth, siderophores of both microbial and plant origin play a very vital role [159, 162].

Potential biocontrol agent

Siderophores have an important role in controlling pathogens affecting plants. Siderophores hold large amounts of iron leading to the reduced accessibility of iron for other microbes in the habitat, which even include the plant pathogenic bacteria. With this strategy, they are helping plants in combating their pathogens [51, 163]. Many researchers have reported the biocontrol agent application of siderophores. The usage of chemical fertilizer and synthetic fungicides can be minimized, as siderophores are natural nontoxic products of bacteria [158]. In 1980, Kloepper et al. raised the curtain unveiling the potential of siderophore for being used as a biological application. Kloepper et al. used different strains of *P. fluorescens* (like TL3B1, A1, B10, and BK1) for confronting *Erwinia carotovora* infection [157]. *Fusarium oxysporum* causes wilt disease in potato, which can be controlled by PVD, a siderophore produced by *Pseudomonads* sp. bacteria [164]. *Gaeumannomyces graminis* is a pathogenic fungus that causes damages barley and wheat crops mainly [165].

The siderophore PVD is very much active against it and shields the plant from its pathogenic effects. Not only in barley and wheat PVDs are capable of shielding other crops like maize and peanuts [166]. Apart from *Pseudomonads*, even *B. subtilis* is also a producer of siderophores and plays a key role in controlling *F. oxysporum* caused fusarium wilt in pepper [167]. Many fungi, mostly pathogenic to plants depend on Fe^{+3} in the soil for their survival. *Azadirachta indica* produces a cocktail of siderophores which chelate Fe^{+3} and thereby restricting the growth of several pathogenic fungi [168]. In the literature its already been reported by many researchers that siderophores have a capability in inhibiting the plant pathogenic fungi like *Sclerotinia sclerotiorum*, *Phytophthora parasitica*, and *Pythium ultimum* [169, 170]. According to the available and reported literature, siderophores can be considered as potential alternatives for biocontrol agents against many plant pathogens.

Nanotechnology, NPs, and Siderophores

Nanotechnology involves the manipulation and utilization of materials at the nanoscale, typically at dimensions less than 100 nm [171-173]. NPs, which are particles with sizes in the nanoscale range, play a central role in nanotechnology [174-176]. Siderophores, on the other hand, are small molecules produced by microorganisms, including bacteria and fungi, to scavenge and transport iron from the environment

[177]. These molecules have a high affinity for iron and are involved in the microbial acquisition of this essential nutrient [178]. In the context of NPs synthesis, siderophores can play a crucial role in the formation and stabilization of NPs, especially those containing metals like iron. The intersection of nanotechnology, NPs, and siderophores brings forth interesting possibilities and applications. The following are the few advantages offered by the use of siderophores in NPs synthesis.

Metal ion chelation

Siderophores can chelate metal ions, including iron [178]. In NPs synthesis, this property is exploited to bind metal ions and create a controlled environment for NPs formation. The binding of metal ions by siderophores helps in the nucleation and growth of NPs. Once siderophores bind to metal ions, the resulting complexes can act as precursors for NPs nucleation and growth. The metal ions within the siderophore complex serve as the building blocks for the formation of NPs.

Bio-mineralization

Siderophores can act as templates for the bio-mineralization of NPs. The metal ions chelated by siderophores can undergo controlled precipitation and nucleation processes, leading to the formation of NPs with well-defined sizes and shapes.

Stabilization

Siderophores can also act as stabilizing agents for NPs. The organic nature of siderophores provides a coating around the NPs, preventing them from agglomerating or precipitating. This stabilization is important for maintaining the colloidal stability and dispersibility of NPs.

Environmentally friendly synthesis

The use of siderophores in NPs synthesis can be considered environmentally friendly. Siderophores are natural products, and their application in NPs synthesis can reduce the reliance on synthetic and potentially harmful stabilizing agents.

Biological applications

Siderophore-mediated synthesis of NPs can be particularly useful for biomedical applications. The resulting NPs can be designed for drug delivery, imaging, or other therapeutic purposes. The biocompatibility of siderophores can make the nanoparticles suitable for various biological applications.

It's worth noting that the field of NPs synthesis is broad and diverse, and researchers continually explore innovative approaches. The use of natural products like siderophores adds a bioinspired dimension to the synthesis process, offering new possibilities for controlled and environmentally friendly NPs production (Table 4).

Siderophores Based NPs as Antimicrobial Agents

The challenge of drug resistance in microbes could find a solution through the application of nanotechnology [188-190]. Nanomaterials, which can be metallic, semiconducting, polymer, or carbon-based, have been extensively investigated

Table 4: Siderophores based NPs synthesis and their applications reported in literature.

Source	Siderophore	NPs type	Properties	Outcome	Ref.
Synthesized	Tripodal catecholates	Zinc oxide	Spherical and 25 nm	immobilization of tripodal PEG-catecholates on NPs	[179]
Synthesized	DFO B	Silver	450 nm (λ_{max})	AgNPs functionalized with DFO b derived ligand for Fe ³⁺ binding and sensing	[180]
Isolated from <i>Escherichia coli</i> Nissle 1917	Delftibactin, Enterobactin, Aerobactin, and Yersiniabactin	Gold	600 nm (λ_{max})	NPs formation by microbial metal-lophores (hydroxamates, catechols, citrates, and mixed ligands)	[181]
Extracted from <i>P. aeruginosa</i> DM1	PVD	Zinc oxide	362 nm (λ_{max}), polycrystalline wurtzite, 50 to 100 nm	Broad spectrum antimicrobial effects	[182]
Synthesized	2,3-dihydroxybenzoylglycine	Iron oxide	Crystalline, 9.8 ± 1.8 nm, ~7.2 ± 1 nm	Showed highly selective and sensitive fluorimetric detection of Al ³⁺ in water at physiological pH	[91]
Isolated from <i>P. aeruginosa</i> 25W	PVD	Gold	550 nm (λ_{max}), FCC, triangular and hexagonal, 50 nm and 2 μ m	NPs showed potent anticancer activity against metastatic A549 lung cancer cells	[183]
		Silver	425 nm (λ_{max}), FCC, irregular shape, 50 to 100 nm		
Synthesized	Feroxamine	Iron oxide@silicon dioxide@amine	Crystalline, 22.14 mV, ~10 nm	Electrostatic surface interactions between NP conjugate and ferroxamine receptor for pathogen (<i>Yersinia enterocolitica</i> wild type) detection	[184]

and demonstrated their effectiveness against infections listed as priorities by the World Health Organization [191]. The antimicrobial properties of nanomaterials result from their interactions with microbe, involving processes such as cellular uptake and NPs aggregation, which in turn leads to membrane damage and toxicity [192, 193]. To mitigate antibiotic resistant microbes, NPs can function both as antibiotics and delivery systems [194, 195]. In the context of antibacterial agents, NPs can be designed and engineered to exhibit antimicrobial properties, making them effective against bacteria [196-198].

Kotb et al. reported the conjugation of PVDs with iron NPs and their antibacterial potential was studied against few Gram-negative bacteria. Results also indicated that the conjugates enter the bacterial cell through the ferriPVDs uptake pathway, initiating the accumulation of iron NPs within the cell, a critical factor for bacterial viability [199]. Certain nanoparticles, like magnetite (Fe₃O₄) NPs, can penetrate Gram-negative bacteria via the siderophore channels present on the outer membrane. These NPs have the potential to act as “Trojan horses,” facilitating the transfer of nano-coupled antibiotics that are typically hindered by the outer membrane, into Gram-negative bacteria [200, 201].

Siderophores Based NPs as Anticancer Agents

Siderophores have recently ushered in new opportunities in the field of nanomedicine. In the strategy for treating cancer, siderophores can limit the availability of iron to cancer cells [202].

Nosrati et al. reported the integration of a theranostic agent for tumor diagnosis and targeted delivery of anti-cancer drugs can be achieved by combining a SPIONPs-siderophore conjugate with MUC1_{Apt} as a targeting molecule and DOX as the chemotherapeutic drug. The targeted drug delivery system

(SPION/PVD/MUC1_{Apt}/DOX) was created by covalently attaching the SPION/PVD complex to MUC1_{Apt} and incorporating DOX into the formulation. The examination of cellular cytotoxicity and uptake of formulations using MTT and flow cytometry in both MUC1-negative (CHO) and MUC1-positive (C26) cell lines demonstrated that MUC1_{Apt} enhanced both cellular uptake and toxicity specifically in the C26 cell line. The assessment of tumor-targeting efficacy through *in vivo* bio-distribution indicated that the targeted formulation could augment the inhibitory effect on tumor growth and improve survival rates in C26 tumor-bearing mice. Additionally, the potential of the synthesized SPION/PVD/MUC1_{Apt}/DOX complex as a diagnostic agent was explored through MRI, enhancing the contrast at the tumor site in MRI scans [202].

Siderophores Based NPs as Heavy Metal Sensors

Heavy metals contribute significantly to environmental pollution, given their widespread presence and resistance to degradation in the environment. The analysis of trace levels of highly toxic heavy metals such as Ar, Pb, Hg, and Cd reveals their potential to pose various health hazards to humans. In order to develop rapid, highly sensitive techniques for analyzing ultra-trace amounts of heavy metals in diverse environmental and biological samples, innovative biosensors have been created through the incorporation of strategies derived from nano-biotechnology [203].

Siderophores Based NPs as Biosensors

Siderophores-based NPs have gained attention in the development of biosensors due to their unique properties and potential applications in detecting specific analytes [200].

Wang et al. designed and developed a triple-module bi-

osensor. The first module consists of Ca²⁺-doped superparamagnetic NPs modified with an aptamer specific to *Helicobacter pylori*, serving the purpose of selectively capturing *H. pylori* cells from samples. The second module is a bifunctional co-polymer containing chloroporphyrin IX Fe³⁺, polyethylene glycol, and DFO, capable of binding to *H. pylori* with high affinity. This co-polymer also chelates Fe³⁺ from the third module, which comprises Fe³⁺-quenched carbon dots solution [204]. Cámara-Martos et al. reported method for detecting Fe³⁺ in wine involves utilizing a single-walled carbon nanotube field-effect transistor immunoassay that is modified with transferrin antibodies. In this setup, the transferrin antibodies are immobilized non-covalently and absorbed directly into the channel area of the single-walled carbon nanotube field-effect transistor. The sensing mechanism of this sensor relies on the chelation interaction between Fe³⁺ and the chelating ligands present in siderophores, resulting in the formation of Fe³⁺-siderophores complexes [205].

Conclusion and Future Perspectives

Actinomycetes are well-acknowledged for the production of industrially and medicinally important bioactive secondary metabolites. The microbial and mineral interactions play a significant role in making the earth more suitable for living forms. Under iron limited conditions, microorganisms produce siderophores. Siderophores have a broad spectrum of applications in various fields including agriculture, medicine, bioremediation, siderotyping, and biosensors but research in the fields of microbiology are yet to be explored. In medicine, to treat the iron-overload diseases and as delivery vehicles for drugs or antibiotics, siderophores are commonly used. Compared to terrestrial, only a handful of marine siderophores were reported to date. The identification and characterization of simple organic structures in complex samples present unique challenges. Using high throughput techniques especially, HPLC, HR-ESI-MS possibly in combination with NMR, to characterize and determine the structure of novel siderophores even if the quantity of sample is lesser. The functional and structural characteristics of siderophores are to be investigated to understand the relationship between microbial communities and siderophores, which can be helpful to improve the new application of siderophore in metal remediation. There is much need to identify the siderophores from extremophiles in marine surface and deep waters, forest, and desert ecosystems to improve and develop the current applications for the welfare human as well as the environment. The combination of nanotechnology, nanoparticles, and siderophores opens up avenues for innovative and sustainable applications across various fields, from medicine to environmental science. The unique properties of siderophores contribute to the design of functionalized nanoparticles with specific and valuable characteristics.

Acknowledgements

Authors thank the Director, National Institute of Technology-Warangal (Telangana, India) and M.H.R.D. for providing the fellowship.

Conflict of Interest

None.

References

1. Khan A, Singh P, Srivastava A. 2018. Synthesis, nature and utility of universal iron chelator-siderophore: a review. *Microbiol Res* 212: 103-111. <https://doi.org/10.1016/j.micres.2017.10.012>
2. Acquah KS, Beukes DR, Warner DF, Meyers PR, Sunassee SN, et al. 2020. Novel South African rare actinomycete *Kribbella speibonae* strain SK5: a prolific producer of hydroxamate siderophores including new dehydroxylated congeners. *Molecules* 25(13): 2979. <https://doi.org/10.3390/molecules25132979>
3. Neilands JB. 1995. Siderophores: structure and function of microbial iron transport compounds. *J Biol Chem* 270(45): 26723-26726. <https://doi.org/10.1074/jbc.270.45.26723>
4. Bergeron RJ, Huang G, Smith RE, Bharti N, McManis JS, et al. 2003. Total synthesis and structure revision of petrobactin. *Tetrahedron* 59(11): 2007-2014. [https://doi.org/10.1016/S0040-4020\(03\)00103-0](https://doi.org/10.1016/S0040-4020(03)00103-0)
5. Holinsworth B, Martin JD. 2009. Siderophore production by marine-derived fungi. *Biometals* 22: 625-632. <https://doi.org/10.1007/s10534-009-9239-y>
6. Sandy M, Butler A. 2009. Microbial iron acquisition: marine and terrestrial siderophores. *Chem Rev* 109(10): 4580-4595. <https://doi.org/10.1021/cr9002787>
7. Devireddy LR, Hart DO, Goetz DH, Green MR. 2010. A mammalian siderophore synthesized by an enzyme with a bacterial homolog involved in enterobactin production. *Cell* 141(6): 1006-1017. <https://doi.org/10.1016/j.cell.2010.04.040>
8. Nagoba B, Vedpathak DV. 2011. Medical applications of siderophores—a review. *Eur J Gen Med* 8(3): 230-233. <https://doi.org/10.29333/ejgm/82743>
9. Imada C, Koseki N, Kamata M, Kobayashi T, Hamada-Sato N. 2007. Isolation and characterization of antibacterial substances produced by marine actinomycetes in the presence of seawater. *Actinomycetologica* 21(1): 27-31. <https://doi.org/10.3209/saj.SAJ210104>
10. Jensen PR, Fenical W. 1994. Strategies for the discovery of secondary metabolites from marine bacteria: ecological perspectives. *Ann Rev Microbiol* 48(1): 559-584. <https://doi.org/10.1146/annurev.mi.48.100194.003015>
11. Zhang L, An R, Wang J, Sun N, Zhang S, et al. 2005. Exploring novel bioactive compounds from marine microbes. *Curr Opin Microbiol* 8(3): 276-281. <https://doi.org/10.1016/j.mib.2005.04.008>
12. Ramesh S, Mathivanan N. 2009. Screening of marine actinomycetes isolated from the Bay of Bengal, India for antimicrobial activity and industrial enzymes. *World J Microbiol Biotechnol* 25: 2103-2111. <https://doi.org/10.1007/s11274-009-0113-4>
13. Liermann LJ, Kalinowski BE, Brantley SL, Ferry JG. 2000. Role of bacterial siderophores in dissolution of hornblende. *Geochim Cosmochim Acta* 64(4): 587-602. [https://doi.org/10.1016/S0016-7037\(99\)00288-4](https://doi.org/10.1016/S0016-7037(99)00288-4)
14. Francis J, Madinaveitia J, Macturk HM, Snow GA. 1949. Isolation from acid-fast bacteria of a growth-factor for *Mycobacterium johnei* and of a precursor of phthiocol. *Nature* 163(4140): 365-366. <https://doi.org/10.1038/163365b0>
15. Hesseltine CW, Pidacks C, Whitehill AR, Bohonos N, Hutchings BL, et al. 1952. Coprogen, a new growth factor for coprophilic fungi. *J Am Chem Soc* 74(5): 1362-1362. <https://doi.org/10.1021/ja01125a525>
16. Neilands JB. 1952. A crystalline organo-iron pigment from a rust fungus (*Ustilago sphaerogena*). *J Am Chem Soc* 74(19): 4846-4847. <https://doi.org/10.1021/ja01139a033>
17. Garibaldi JA, Neilands JB. 1956. Formation of iron-binding compounds by micro-organisms. *Nature* 177(4507): 526-527. <https://doi.org/10.1038/177526a0>

18. de Carvalho CCCR, Marques MPC, Fernandes P. 2011. Recent achievements on siderophore production and application. *Recent Pat Biotechnol* 5(3): 183-198. <https://doi.org/10.2174/187220811797579114>
19. Wilde EJ, Blagova EV, Sanderson TJ, Raines DJ, Thomas RP, et al. 2019. Mimicking salmochelin S1 and the interactions of its Fe(III) complex with periplasmic iron siderophore binding proteins CeuE and VctP. *J Inorg Biochem* 190: 75-84. <https://doi.org/10.1016/j.jinorgbio.2018.10.008>
20. Matzanke BF, Anemüller S, Schünemann V, Trautwein AX, Hantke K. 2004. PhuF, part of a siderophore-reductase system. *Biochemistry* 43(5): 1386-1392. <https://doi.org/10.1021/bi0357661>
21. Martinez JS, Butler A. 2007. Marine amphiphilic siderophores: marinobactin structure, uptake, and microbial partitioning. *J Inorg Biochem* 101(11-12): 1692-1698. <https://doi.org/10.1016/j.jinorgbio.2007.07.007>
22. Martinez JS, Carter-Franklin JN, Mann EL, Martin JD, Haygood MG, et al. 2003. Structure and membrane affinity of a suite of amphiphilic siderophores produced by a marine bacterium. *Proc Natl Acad Sci* 100(7): 3754-3759. <https://doi.org/10.1073/pnas.0637444100>
23. Owen T, Pynn R, Martinez JS, Butler A. 2005. Micelle-to-vesicle transition of an iron-chelating microbial surfactant, marinobactin E. *Langmuir* 21(26): 12109-12114. <https://doi.org/10.1021/la0519352>
24. Saha M, Sarkar S, Sarkar B, Sharma BK, Bhattacharjee S, et al. 2016. Microbial siderophores and their potential applications: a review. *Environ Sci Pollut Res* 23: 3984-3999. <https://doi.org/10.1007/s11356-015-4294-0>
25. Dave BP, Anshuman K, Hajela P. 2006. Siderophores of halophilic archaea and their chemical characterization. *Indian J Exp Biol* 44: 340-344.
26. Nielsen A, Mansson M, Wietz M, Varming AN, Phipps RK, et al. 2012. Nigribactin, a novel siderophore from *Vibrio nigripulchritudo*, modulates *Staphylococcus aureus* virulence gene expression. *Mar Drugs* 10(11): 2584-2595. <https://doi.org/10.3390/md10112584>
27. Pérez-Miranda S, Cabirol N, George-Téllez R, Zamudio-Rivera LS, Fernández FJ. 2007. O-CAS, a fast and universal method for siderophore detection. *J Microbiol Methods* 70(1): 127-131. <https://doi.org/10.1016/j.mimet.2007.03.023>
28. Vraspir JM, Holt PD, Butler A. 2011. Identification of new members within suites of amphiphilic marine siderophores. *Biomaterials* 24: 85-92. <https://doi.org/10.1007/s10534-010-9378-1>
29. Homann VV, Sandy M, Tincu JA, Templeton AS, Tebo BM, et al. 2009. Loihichelins A-F, a suite of amphiphilic siderophores produced by the marine bacterium *Halomonas* LOB-5. *J Nat Prod* 72(5): 884-888. <https://doi.org/10.1021/np800640h>
30. Shenker M, Oliver I, Helmann M, Hadar Y, Chen Y. 1992. Utilization by tomatoes of iron mediated by a siderophore produced by *Rhizopus arrhizus*. *J Plant Nutr* 15(10): 2173-2182. <https://doi.org/10.1080/01904169209364466>
31. Barbeau K, Zhang G, Live DH, Butler A. 2002. Petrobactin, a photoreactive siderophore produced by the oil-degrading marine bacterium *Marinobacter hydrocarbonoclasticus*. *J Am Chem Soc* 124(3): 378-379. <https://doi.org/10.1021/ja0119088>
32. Hickford SJ, Küpper FC, Zhang G, Carrano CJ, Blunt JW, et al. 2004. Petrobactin sulfonate, a new siderophore produced by the marine bacterium *Marinobacter hydrocarbonoclasticus*. *J Nat Prod* 67(11): 1897-1899. <https://doi.org/10.1021/np049823i>
33. Kanoh K, Kamino K, Leleo G, Adachi K, Shizuri Y. 2003. Pseudoalterobactin A and B, new siderophores excreted by marine bacterium *Pseudoalteromonas* sp. KP20-4. *J Antibiot* 56(10): 871-875. <https://doi.org/10.7164/antibiotics.56.871>
34. Wang W, Qiu Z, Tan H, Cao L. 2014. Siderophore production by actinobacteria. *Biomaterials* 27: 623-631. <https://doi.org/10.1007/s10534-014-9739-2>
35. You JL, Cao LX, Liu GF, Zhou SN, Tan HM, et al. 2005. Isolation and characterization of actinomycetes antagonistic to pathogenic *Vibrio* spp. from nearshore marine sediments. *World J Microbiol Biotechnol* 21: 679-682. <https://doi.org/10.1007/s11274-004-3851-3>
36. Matsuo Y, Kanoh K, Jang JH, Adachi K, Matsuda S, et al. 2011. Streptobactin, a tricatechol-type siderophore from marine-derived *Streptomyces* sp. YM5-799. *J Nat Prod* 74(11): 2371-2376. <https://doi.org/10.1021/np200290j>
37. Stoll A, Brack A, Renz J. 1951. Nocardamin, ein neues antibiotikum aus einer Nocardia-Art. *Pathobiology* 14(2): 225-233. <https://doi.org/10.1159/000159979>
38. Kalinovskaya NI, Romanenko LA, Irisawa T, Ermakova SP, Kalinovskiy AI. 2011. Marine isolate *Citricoccus* sp. KMM 3890 as a source of a cyclic siderophore nocardamine with antitumor activity. *Microbiol Res* 166(8): 654-661. <https://doi.org/10.1016/j.micres.2011.01.004>
39. Eje N, Soe CZ, Gu J, Codd R. 2013. The variable hydroxamic acid siderophore metabolome of the marine actinomycete *Salinispora tropica* CNB-440. *Metallomics* 5(11): 1519-1528. <https://doi.org/10.1039/c3mt00230f>
40. Liu N, Shang F, Xi L, Huang Y. 2013. Tetroazolemycins A and B, two new oxazole-thiazole siderophores from deep-sea *Streptomyces olivaceus* FXJ8. 012. *Mar Drugs* 11(5): 1524-1533. <https://doi.org/10.3390/md11051524>
41. Takehana Y, Umekita M, Hatano M, Kato C, Sawa R, et al. 2017. Fradiamine A, a new siderophore from the deep-sea actinomycete *Streptomyces fradiae* MM456M-mF7. *J Antibiot* 70(5): 611-615. <https://doi.org/10.1038/ja.2017.26>
42. Yang M, Zhang J, Liang Q, Pan G, Zhao J, et al. 2019. Antagonistic activity of marine *Streptomyces* sp. S073 on pathogenic *Vibrio parahaemolyticus*. *Fish Sci* 85: 533-543. <https://doi.org/10.1007/s12562-019-01309-z>
43. Wu Q, Deering RW, Zhang G, Wang B, Li X, et al. 2018. Albisporachelin, a new hydroxamate type siderophore from the deep ocean sediment-derived actinomycete *Amycolatopsis albispora* WP1T. *Mar Drugs* 16(6): 199. <https://doi.org/10.3390/md16060199>
44. Yan JX, Chevrette MG, Braun DR, Harper MK, Currie CR, et al. 2019. Madurastatin D1 and D2, oxazoline containing siderophores isolated from an *Actinomadura* sp. *Org Lett* 21(16): 6275-6279. <https://doi.org/10.1021/acs.orglett.9b02159>
45. Neilands JB. 1981. Microbial iron compounds. *Annu Rev Biochem* 50(1): 715-731. <https://doi.org/10.1146/annurev.bi.50.070181.003435>
46. Winkelmann G. 2002. Microbial siderophore-mediated transport. *Biochem Soc Trans* 30(4): 691-696. <https://doi.org/10.1042/bst0300691>
47. Ballouche M, Cornelis P, Baysse C. 2009. Iron metabolism: a promising target for antibacterial strategies. *Recent Pat Antiinfect Drug Discov* 4: 190-205. <https://doi.org/10.2174/157489109789318514>
48. Dmitriev BA, Toukach FV, Schaper KJ, Holst O, Rietschel ET, et al. 2003. Tertiary structure of bacterial murein: the scaffold model. *J Bacteriol* 185(11): 3458-3468. <https://doi.org/10.1128/jb.185.11.3458-3468.2003>
49. Krewulak KD, Vogel HJ. 2008. Structural biology of bacterial iron uptake. *Biochim Biophys Acta Biomembr* 1778(9): 1781-1804. <https://doi.org/10.1016/j.bbamem.2007.07.026>
50. Miethke M, Marahiel MA. 2007. Siderophore-based iron acquisition and pathogen control. *Microbiol Mol Biol Rev* 71(3): 413-451. <https://doi.org/10.1128/mmbr.00012-07>
51. Ahmed E, Holmström SJ. 2014. Siderophores in environmental research: roles and applications. *Microb Biotechnol* 7(3): 196-208. <https://doi.org/10.1111/1751-7915.12117>
52. Beger RD. 2013. A review of applications of metabolomics in cancer. *Metabolites* 3(3): 552-574. <https://doi.org/10.3390/metabo3030552>
53. Mastrangelo A, Armitage EG, García A, Barbas C. 2014. Metabolomics as a tool for drug discovery and personalised medicine. A review.

- Curr Top Med Chem* 14(23): 2627-2636. <https://doi.org/10.2174/1568026614666141215124956>
54. Zwiener C, Frimmel FH. 2004. LC-MS analysis in the aquatic environment and in water treatment technology—a critical review: part II: applications for emerging contaminants and related pollutants, micro-organisms and humic acids. *Anal Bioanal Chem* 378: 862-874. <https://doi.org/10.1007/s00216-003-2412-1>
 55. Patti GJ, Yanes O, Siuzdak G. 2012. Metabolomics: the apogee of the omics trilogy. *Nat Rev Mol Cell Biol* 13(4): 263-269. <https://doi.org/10.1038/nrm3314>
 56. Carmichael JR, Zhou H, Butler A. 2019. A suite of asymmetric citrate siderophores isolated from a marine *Shewanella* species. *J Inorg Biochem* 198: 110736. <https://doi.org/10.1016/j.jinorgbio.2019.110736>
 57. Sester A, Winand L, Pace S, Hiller W, Werz O, et al. 2019. Myxochelin- and pseudochelin-derived lipoxygenase inhibitors from a genetically engineered *Myxococcus xanthus* strain. *J Nat Prod* 82(9): 2544-2549. <https://doi.org/10.1021/acs.jnatprod.9b00403>
 58. Diettrich J, Kage H, Nett M. 2019. Genomics-inspired discovery of massiliachelin, an agrochelin epimer from *Massilia* sp. NR 4-1. *Beilstein J Org Chem* 15(1): 1298-1303. <https://doi.org/10.3762/bjoc.15.128>
 59. Hardy CD, Butler A. 2019. Ambiguity of NRPS structure predictions: four bidentate chelating groups in the siderophore pacifibactin. *J Nat Prod* 82(4): 990-997. <https://doi.org/10.1021/acs.jnatprod.8b01073>
 60. Robertson AW, McCarville NG, MacIntyre LW, Correa H, Haltli B, et al. 2018. Isolation of imaobactin, an amphiphilic siderophore from the arctic marine bacterium *Variovorax* species RKJM285. *J Nat Prod* 81(4): 858-865. <https://doi.org/10.1021/acs.jnatprod.7b00943>
 61. Sonnenschein EC, Stierhof M, Goralczyk S, Vabre FM, Pellissier L, et al. 2017. Pseudochelin A, a siderophore of *Pseudoalteromonas piscicida* S2040. *Tetrahedron* 73(18): 2633-2637. <https://doi.org/10.1016/j.tet.2017.03.051>
 62. Zhang F, Barns K, Hoffmann FM, Braun DR, Andes DR, et al. 2017. Thalassosamide, a siderophore discovered from the marine-derived bacterium *Thalassospira profundimaris*. *J Nat Prod* 80(9): 2551-2555. <https://doi.org/10.1021/acs.jnatprod.7b00328>
 63. Kurth C, Schieferdecker S, Athanasopoulou K, Seccareccia I, Nett M. 2016. Variochelins, lipopeptide siderophores from *Variovorax boronicumulans* discovered by genome mining. *J Nat Prod* 79(4): 865-872. <https://doi.org/10.1021/acs.jnatprod.5b00932>
 64. Fujita MJ, Sakai R. 2014. Production of avaroferrin and putrebactin by heterologous expression of a deep-sea metagenomic DNA. *Mar Drugs* 12(9): 4799-4809. <https://doi.org/10.3390/md12094799>
 65. Gauglitz JM, Butler A. 2013. Amino acid variability in the peptide composition of a suite of amphiphilic peptide siderophores from an open ocean *Vibrio* species. *J Biol Inorg Chem* 18: 489-497. <https://doi.org/10.1007/s00775-013-0995-3>
 66. Gauglitz JM, Zhou H, Butler A. 2012. A suite of citrate-derived siderophores from a marine *Vibrio* species isolated following the deep-water horizon oil spill. *J Inorg Biochem* 107(1): 90-95. <https://doi.org/10.1016/j.jinorgbio.2011.10.013>
 67. Ito Y, Butler A. 2005. Structure of synechobactins, new siderophores of the marine cyanobacterium *Synechococcus* sp. PCC 7002. *Limnol Oceanogr* 50(6): 1918-1923. <https://doi.org/10.4319/lo.2005.50.6.1918>
 68. Martinez JS, Haygood MG, Butler A. 2001. Identification of a natural desferrioxamine siderophore produced by a marine bacterium. *Limnol Oceanogr* 46(2): 420-424. <https://doi.org/10.4319/lo.2001.46.2.0420>
 69. Martinez JS, Zhang GP, Holt PD, Jung HT, Carrano CJ, et al. 2000. Self-assembling amphiphilic siderophores from marine bacteria. *Science* 287(5456): 1245-1247. <https://doi.org/10.1126/science.287.5456.1245>
 70. Zhao W, Peng F, Wang CX, Xie Y, Lin R, et al. 2020. FW0622, a new siderophore isolated from marine *Verrucosisspora* sp. by genomic mining. *Nat Prod Res* 34(21): 3082-3088. <https://doi.org/10.1080/14786419.2019.1608541>
 71. Walker LR, Tfaily MM, Shaw JB, Hess NJ, Paša-Tolić L, et al. 2017. Unambiguous identification and discovery of bacterial siderophores by direct injection 21 Tesla fourier transform ion cyclotron resonance mass spectrometry. *Metallomics* 9(1): 82-92. <https://doi.org/10.1039/c6mt00201c>
 72. Ledyard KM, Butler A. 1997. Structure of putrebactin, a new dihydroxamate siderophore produced by *Shewanella putrefaciens*. *J Biol Inorg Chem* 2: 93-97. <https://doi.org/10.1007/s007750050110>
 73. Jalal MAF, Hossain MB, Van der Helm D, Sanders-Loehr J, Actis LA, et al. 1989. Structure of anguibactin, a unique plasmid-related bacterial siderophore from the fish pathogen *Vibrio anguillarum*. *J Am Chem Soc* 111(1): 292-296. <https://doi.org/10.1021/ja00183a044>
 74. Takahashi A, Nakamura H, Kameyama T, Kurasawa S, Naganawa H, et al. 1987. Bisucaberin, a new siderophore, sensitizing tumor cells to macrophage-mediated cytotoxicity II. Physico-chemical properties and structure determination. *J Antibiot* 40(12): 1671-1676. <https://doi.org/10.7164/antibiotics.40.1671>
 75. Zhang L, Yuan DX, Fang K, Liu BM. 2015. Determination of siderophores in seawater by high performance liquid chromatography-tandem mass spectrometry coupled with solid phase extraction. *Chinese J Anal Chem* 43(9): 1285-1290. [https://doi.org/10.1016/S1872-2040\(15\)60854-4](https://doi.org/10.1016/S1872-2040(15)60854-4)
 76. Clark CM, Costa MS, Sanchez LM, Murphy BT. 2018. Coupling MALDI-TOF mass spectrometry protein and specialized metabolite analyses to rapidly discriminate bacterial function. *Proc Natl Acad Sci* 115(19): 4981-4986. <https://doi.org/10.1073/pnas.1801247115>
 77. Gáll T, Lehoczki G, Gyémánt G, Emri T, Szigeti ZM, et al. 2016. Optimization of desferrioxamine E production by *Streptomyces parvulus*. *Acta Microbiol Immunol Hung* 63(4): 475-489. <https://doi.org/10.1556/030.63.2016.029>
 78. Guerrero-Garzon JF, Zehl M, Schneider O, Rückert C, Busche T, et al. 2020. *Streptomyces* spp. from the marine sponge *Antho dichotoma*: analyses of secondary metabolite biosynthesis gene clusters and some of their products. *Front Microbiol* 11: 437. <https://doi.org/10.3389/fmicb.2020.00437>
 79. Vigneshvar S, Sudhakumari CC, Senthilkumaran B, Prakash H. 2016. Recent advances in biosensor technology for potential applications—an overview. *Front Bioeng Biotechnol* 4: 11. <https://doi.org/10.3389/fbioe.2016.00011>
 80. Gupta V, Saharan K, Kumar L, Gupta R, Sahai V, et al. 2008. Spectrophotometric ferric ion biosensor from *Pseudomonas fluorescens* culture. *Biotechnol Bioeng* 100(2): 284-296. <https://doi.org/10.1002/bit.21754>
 81. Mokhtarzadeh A, Dolatabadi JEN, Abnous K, de la Guardia M, Ramezani M. 2015. Nanomaterial-based cocaine aptasensors. *Biosens Bioelectron* 68: 95-106. <https://doi.org/10.1016/j.bios.2014.12.052>
 82. Nosrati R, Golichenari B, Nezami A, Taghdisi SM, Karimi B, et al. 2017. *Helicobacter pylori* point-of-care diagnosis: nano-scale biosensors and microfluidic systems. *TrAC Trends Anal Chem* 97: 428-444. <https://doi.org/10.1016/j.trac.2017.10.013>
 83. Nosrati R, Dehghani S, Karimi B, Yousefi M, Taghdisi SM, et al. 2018. Siderophore-based biosensors and nanosensors; new approach on the development of diagnostic systems. *Biosens Bioelectron* 117: 1-14. <https://doi.org/10.1016/j.bios.2018.05.057>
 84. Yin K, Wu Y, Wang S, Chen L. 2016. A sensitive fluorescent biosensor for the detection of copper ion inspired by biological recognition element pyoverdine. *Sens Actuators B Chem* 232: 257-263. <https://doi.org/10.1016/j.snb.2016.03.128>
 85. Chung Chun Lam CK, Jickells TD, Richardson DJ, Russell DA. 2006. Fluorescence-based siderophore biosensor for the determination of bioavailable iron in oceanic waters. *Anal Chem* 78(14): 5040-5045. <https://doi.org/10.1021/ac060223t>
 86. Orcutt KM, Jones WS, McDonald A, Schrock D, Wallace K J. 2010. A lanthanide-based chemosensor for bioavailable Fe³⁺ using a fluorescent siderophore: an assay displacement approach. *Sensors* 10(2): 1326-1337. <https://doi.org/10.3390/s100201326>

87. Phillips DJ, Davies GL, Gibson MI. 2015. Siderophore-inspired nanoparticle-based biosensor for the selective detection of Fe³⁺. *J Mater Chem B* 3(2): 270-275. <https://doi.org/10.1039/c4tb01501k>
88. Sharma M, Gohil NK. 2010. Optical features of the fluorophore azotobactin: applications for iron sensing in biological fluids. *Eng Life Sci* 10(4): 304-310. <https://doi.org/10.1002/elsc.201000038>
89. Yoder MF, Kisaalita WS. 2011. Iron specificity of a biosensor based on fluorescent pyoverdine immobilized in sol-gel glass. *J Biol Eng* 5(1): 1-12. <https://doi.org/10.1186/1754-1611-5-4>
90. Raju M, Nair RR, Raval IH, Haldar S, Chatterjee PB. 2018. A water soluble Cu²⁺-specific colorimetric probe can also detect Zn²⁺ in live shrimp and aqueous environmental samples by fluorescence channel. *Sens Actuators B Chem* 260: 364-370. <https://doi.org/10.1016/j.snb.2018.01.010>
91. Raju M, Srivastava S, Nair RR, Raval IH, Haldar S, et al. 2017. Siderophore coated magnetic iron nanoparticles: rational designing of water soluble nanobiosensor for visualizing Al³⁺ in live organism. *Biosens Bioelectron* 97: 338-344. <https://doi.org/10.1016/j.bios.2017.06.013>
92. Duhme-Klair AK. 2009. From siderophores and self-assembly to luminescent sensors: the binding of molybdenum by catecholamides. *Eur J Inorg Chem* 2009(25): 3689-3701. <https://doi.org/10.1002/ejic.200900416>
93. Duhme-Klair AK, de Alwis DCL, Schultz FA. 2003. Electrochemistry of molybdenum(VI)-catecholamide siderophore complexes in aqueous solution. *Inorg Chim Acta* 351: 150-158. [https://doi.org/10.1016/S0020-1693\(03\)00210-X](https://doi.org/10.1016/S0020-1693(03)00210-X)
94. Jedner SB, Perutz RN, Duhme-Klair AK. 2003. Synthesis and characterization of a siderophore-based luminescent sensor for molybdate. *J Inorg Gen Chem* 629(12-13): 2421-2426. <https://doi.org/10.1002/zaac.200300258>
95. Palanché T, Marmolle F, Abdallah MA, Shanzer A, Albrecht-Gary AM. 1999. Fluorescent siderophore-based chemosensors: iron(III) quantitative determinations. *J Biol Inorg Chem* 4: 188-198. <https://doi.org/10.1007/s007750050304>
96. Visca P, Imperi F, Lamont IL. 2007. Pyoverdine siderophores: from biogenesis to biosignificance. *Trends Microbiol* 15(1): 22-30. <https://doi.org/10.1016/j.tim.2006.11.004>
97. Winkelmann G. 2007. Ecology of siderophores with special reference to the fungi. *Biometals* 20: 379-392. <https://doi.org/10.1007/s10534-006-9076-1>
98. Kraepiel AML, Bellenger JP, Wichard T, Morel FM. 2009. Multiple roles of siderophores in free-living nitrogen-fixing bacteria. *Biometals* 22: 573-581. <https://doi.org/10.1007/s10534-009-9222-7>
99. Yoneyama F, Yamamoto M, Hashimoto W, Murata K. 2011. *Azotobacter vinelandii* gene clusters for two types of peptidic and catechol siderophores produced in response to molybdenum. *J Appl Microbiol* 111(4): 932-938. <https://doi.org/10.1111/j.1365-2672.2011.05109.x>
100. Doorneweerd DD, Henne WA, Reifemberger RG, Low PS. 2010. Selective capture and identification of pathogenic bacteria using an immobilized siderophore. *Langmuir* 26(19): 15424-15429. <https://doi.org/10.1021/la101962w>
101. Bachman MA, Oyler JE, Burns SH, Caza M, Lépine F, et al. 2011. *Klebsiella pneumoniae* yersiniabactin promotes respiratory tract infection through evasion of lipocalin 2. *Infect Immun* 79(8): 3309-3316. <https://doi.org/10.1128/iai.05114-11>
102. Himpf SD, Pearson MM, Arewång CJ, Nusca TD, Sherman DH, et al. 2010. Proteobactin and a yersiniabactin-related siderophore mediate iron acquisition in *Proteus mirabilis*. *Mol Microbiol* 78(1): 138-157. <https://doi.org/10.1111/j.1365-2958.2010.07317.x>
103. Inomata T, Eguchi H, Matsumoto K, Funahashi Y, Ozawa T, et al. 2007. Adsorption of microorganisms onto an artificial siderophore-modified Au substrate. *Biosens Bioelectron* 23(5): 751-755. <https://doi.org/10.1016/j.bios.2007.08.015>
104. Inomata T, Tanabashi H, Funahashi Y, Ozawa T, Masuda H. 2013. Adsorption and detection of *Escherichia coli* using an Au substrate modified with a catecholate-type artificial siderophore-Fe³⁺ complex. *Dalton Trans* 42(45): 16043-16048. <https://doi.org/10.1039/c3dt51448j>
105. Inomata T, Murase T, Ido H, Ozawa T, Masuda H. 2014. Gold Nanoparticles modified with artificial siderophore-iron(III) ion complexes: selective adsorption and aggregation of microbes using "coordination programming". *Chem Lett* 43(7): 1146-1148. <https://doi.org/10.1246/cl.140270>
106. Meyer JM, Stintzi A, De Vos D, Cornelis P, Tappe R, et al. 1997. Use of siderophores to type pseudomonads: the three *Pseudomonas aeruginosa* pyoverdine systems. *Microbiology* 143(1): 35-43. <https://doi.org/10.1099/00221287-143-1-35>
107. Meyer JM, Geoffroy VA, Baida N, Gardan L, Izard D, et al. 2002. Siderophore typing, a powerful tool for the identification of fluorescent and nonfluorescent pseudomonads. *Appl Environ Microbiol* 68(6): 2745-2753. <https://doi.org/10.1128/AEM.68.6.2745-2753.2002>
108. Meyer JM. 2010. Pyoverdine Siderophores as Taxonomic and Phylogenetic Markers. In Ramos J, Filloux A (eds) *Pseudomonas*. Springer, Dordrecht, pp 201-233.
109. Meyer JM, Gruffaz C, Raharinosy V, Bezverbnaya I, Schäfer M, et al. 2008. Siderotyping of fluorescent *Pseudomonas*: molecular mass determination by mass spectrometry as a powerful pyoverdine siderotyping method. *Biometals* 21: 259-271. <https://doi.org/10.1007/s10534-007-9115-6>
110. Bultreys A, Gheysen I, de Hoffmann E. 2006. Yersiniabactin production by *Pseudomonas syringae* and *Escherichia coli*, and description of a second yersiniabactin locus evolutionary group. *Appl Environ Microbiol* 72(6): 3814-3825. <https://doi.org/10.1128/AEM.00119-06>
111. Mokracka J, Koczura R, Kaznowski A. 2004. Yersiniabactin and other siderophores produced by clinical isolates of *Enterobacter* spp. and *Citrobacter* spp. *FEMS Immunol Med Microbiol* 40(1): 51-55. [https://doi.org/10.1016/S0928-8244\(03\)00276-1](https://doi.org/10.1016/S0928-8244(03)00276-1)
112. Kaeberlein T, Lewis K, Epstein SS. 2002. Isolating "uncultivable" microorganisms in pure culture in a simulated natural environment. *Science* 296(5570): 1127-1129. <https://doi.org/10.1126/science.1070633>
113. Lewis K, Epstein S, D'onofrio A, Ling LL. 2010. Uncultured microorganisms as a source of secondary metabolites. *J Antibiot* 63(8): 468-476. <https://doi.org/10.1038/ja.2010.87>
114. Yamanaka K, Oikawa H, Ogawa HO, Hosono K, Shinmachi F, et al. 2005. Desferrioxamine E produced by *Streptomyces griseus* stimulates growth and development of *Streptomyces tanashiensis*. *Microbiology* 151(9): 2899-2905. <https://doi.org/10.1099/mic.0.28139-0>
115. Traxler MF, Seyedsayamdost MR, Clardy J, Kolter R. 2012. Interspecies modulation of bacterial development through iron competition and siderophore piracy. *Mol Microbiol* 86(3): 628-644. <https://doi.org/10.1111/mmi.12008>
116. Huang Y, Jiang Y, Wang H, Wang J, Shin MC, et al. 2013. Curb challenges of the "Trojan Horse" approach: smart strategies in achieving effective yet safe cell-penetrating peptide-based drug delivery. *Adv Drug Deliv Rev* 65(10): 1299-1315. <https://doi.org/10.1016/j.addr.2012.11.007>
117. Miethke M, Marahiel MA. 2007. Siderophore-based iron acquisition and pathogen control. *Microbiol Mol Biol Rev* 71(3): 413-451. <https://doi.org/10.1128/mmbr.00012-07>
118. Möllmann U, Heinisch L, Bauernfeind A, Köhler T, Ankel-Fuchs D. 2009. Siderophores as drug delivery agents: application of the "Trojan Horse" strategy. *Biometals* 22: 615-624. <https://doi.org/10.1007/s10534-009-9219-2>
119. Wenciewicz TA, Möllmann U, Long TE, Miller MJ. 2009. Is drug release necessary for antimicrobial activity of siderophore-drug conjugates? Syntheses and biological studies of the naturally occurring salmycin "Trojan Horse" antibiotics and synthetic desferridanoxamine-antibiotic conjugates. *Biometals* 22: 633-648. <https://doi.org/10.1007/s10534-009-9218-3>

120. Ding P, Schous CE, Miller MJ. 2008. Design and synthesis of a novel protected mixed ligand siderophore. *Tetrahedron Lett* 49(14): 2306-2310. <https://doi.org/10.1016/j.tetlet.2008.02.007>
121. Juárez-Hernández RE, Miller PA, Miller MJ. 2012. Syntheses of siderophore–drug conjugates using a convergent thiol–maleimide system. *ACS Med Chem Lett* 3(10): 799-803. <https://doi.org/10.1021/ml300150y>
122. Ghosh M, Miller MJ. 1996. Synthesis and *in vitro* antibacterial activity of spermidine-based mixed catechol-and hydroxamate-containing siderophore–vancomycin conjugates. *Bioorg Med Chem* 4(1): 43-48. [https://doi.org/10.1016/0968-0896\(95\)00161-1](https://doi.org/10.1016/0968-0896(95)00161-1)
123. Ji C, Miller PA, Miller MJ. 2012. Iron transport-mediated drug delivery: practical syntheses and *in vitro* antibacterial studies of tris-catecholate siderophore–aminopenicillin conjugates reveals selectively potent antipseudomonal activity. *J Am Chem Soc* 134(24): 9898-9901. <https://doi.org/10.1021/ja303446w>
124. Wenczewicz TA, Miller MJ. 2013. Biscatecholate–monohydroxamate mixed ligand siderophore–carbacephalosporin conjugates are selective sideromycin antibiotics that target *Acinetobacter baumannii*. *J Med Chem* 56(10): 4044-4052. <https://doi.org/10.1021/jm400265k>
125. Ferguson AD, Braun V, Fiedler HP, Coulton JW, Diederichs KAY, et al. 2000. Crystal structure of the antibiotic albomycin in complex with the outer membrane transporter FhuA. *Protein Sci* 9(5): 956-963. <https://doi.org/10.1110/ps.9.5.956>
126. Hershko C, Link G, Konijn AM. 2003. Pathophysiology of iron overload-5 cardioprotective effect of iron chelators. *Adv Exp Med Biol* 509: 77-90.
127. Pietrangelo A. 2002. Mechanism of Iron Toxicity. In Hershko C (ed) Iron Chelation Therapy. Advances in Experimental Medicine and Biology. Springer, Boston, pp 19-43.
128. Sah S, Singh R. 2015. Siderophore: structural and functional characterisation - a comprehensive review. *Agriculture* 61(3): 97. <https://doi.org/10.1515/agri-2015-0015>
129. Propper RD, Cooper B, Rufo RR, Nienhuis AW, Anderson WF, et al. 1977. Continuous subcutaneous administration of deferoxamine in patients with iron overload. *New Engl J Med* 297(8): 418-423. <https://doi.org/10.1056/NEJM197708252970804>
130. Robotham JL, Lietman PS. 1980. Acute iron poisoning: a review. *Am J Dis Child* 134(9): 875-879. <https://doi.org/10.1001/archpedi.1980.02130210059016>
131. Summers MR, Jacobs A, Tudway D, Perera P, Ricketts C. 1979. Studies in desferrioxamine and ferrioxamine metabolism in normal and iron-loaded subjects. *Br J Haematol* 42(4): 547-555. <https://doi.org/10.1111/j.1365-2141.1979.tb01167.x>
132. Wilson ME, Britigan BE. 1998. Iron acquisition by parasitic protozoa. *Parasitol Today* 14(9): 348-353. [https://doi.org/10.1016/S0169-4758\(98\)01294-0](https://doi.org/10.1016/S0169-4758(98)01294-0)
133. Lytton SD, Loyevsky M, Mester B, Libman J, et al. 1993. *In vivo* antimalarial action of a lipophilic iron(III) chelator: suppression of *Plasmodium vinckei* infection by reversed siderophore. *Am J Hematol* 43(3): 217-220. <https://doi.org/10.1002/ajh.2830430311>
134. Loyevsky M, John C, Dickens B, Hu V, Miller JH, et al. 1999. Chelation of iron within the erythrocytic *Plasmodium falciparum* parasite by iron chelators. *Mol Biochem Parasitol* 101(1-2): 43-59. [https://doi.org/10.1016/S0166-6851\(99\)00053-5](https://doi.org/10.1016/S0166-6851(99)00053-5)
135. Pradines B, Tall A, Ramiandrasoa F, Spiegel A, Sokhna C, et al. 2006. *In vitro* activity of iron-binding compounds against Senegalese isolates of *Plasmodium falciparum*. *J Antimicrob Chemother* 57(6): 1093-1099. <https://doi.org/10.1093/jac/dkl117>
136. Gauthier JD, Vasta GR. 1994. Inhibition of *in vitro* replication of the oyster parasite *Perkinsus marinus* by the natural iron chelators transferrin, lactoferrin, and desferrioxamine. *Dev Comp Immunol* 18(4): 277-286. [https://doi.org/10.1016/S0145-305X\(94\)90353-0](https://doi.org/10.1016/S0145-305X(94)90353-0)
137. Ackrill P, Ralston AJ, Day JP, Hodge KC. 1980. Successful removal of aluminium from patient with dialysis encephalopathy. *Lancet* 2(8196): 692-693. [https://doi.org/10.1016/s0140-6736\(80\)92728-2](https://doi.org/10.1016/s0140-6736(80)92728-2)
138. Arze RS, Parkinson IS, Carlidge NEF, Britton P, Ward MK. 1981. Reversal of aluminium dialysis encephalopathy after desferrioxamine treatment. *Lancet* 2(8255): 1116. [https://doi.org/10.1016/s0140-6736\(81\)91324-6](https://doi.org/10.1016/s0140-6736(81)91324-6)
139. Hansen TV, Aaseth J, Alexander J. 1982. The effect of chelating agents on vanadium distribution in the rat body and on uptake by human erythrocytes. *Arch Toxicol* 50: 195-202. <https://doi.org/10.1007/BF00310851>
140. Poggitsch H, Petek W, Wawschinek O, Holzer W. 1981. Treatment of early stages of dialysis encephalopathy by aluminium depletion. *Lancet* 2(8259): 1344-1345. [https://doi.org/10.1016/s0140-6736\(81\)91363-5](https://doi.org/10.1016/s0140-6736(81)91363-5)
141. Huang X. 2003. Iron overload and its association with cancer risk in humans: evidence for iron as a carcinogenic metal. *Mutat Res* 533(1-2): 153-171. <https://doi.org/10.1016/j.mrfmmm.2003.08.023>
142. Nakouti I, Sihanonth P, Palaga T, Hobbs G. 2013. Effect of a siderophore producer on animal cell apoptosis: a possible role as anti-cancer agent. *Int J Pharma Med Biol Sci* 2(3): 1-5.
143. Neubauer U, Nowack B, Furrer G, Schulin R. 2000. Heavy metal sorption on clay minerals affected by the siderophore desferrioxamine B. *Environ Sci Technol* 34(13): 2749-2755. <https://doi.org/10.1021/es990495w>
144. Xu S, Xing Y, Liu S, Huang Q, Chen W. 2019. Role of novel bacterial *Raoultella* sp. strain X13 in plant growth promotion and cadmium bioremediation in soil. *Appl Microbiol Biotechnol* 103: 3887-3897. <https://doi.org/10.1007/s00253-019-09700-7>
145. Dimkpa CO, Merten D, Svatoš A, Büchel G, Kothe E. 2009. Siderophores mediate reduced and increased uptake of cadmium by *Streptomyces tendae* F4 and sunflower (*Helianthus annuus*), respectively. *J Appl Microbiol* 107(5): 1687-1696. <https://doi.org/10.1111/j.1365-2672.2009.04355.x>
146. Nair A, Jwarkar AA, Singh SK. 2007. Production and characterization of siderophores and its application in arsenic removal from contaminated soil. *Water Air Soil Pollut* 180: 199-212. <https://doi.org/10.1007/s11270-006-9263-2>
147. Amin SA, Küpper FC, Green DH, Harris WR, Carrano CJ. 2007. Boron binding by a siderophore isolated from marine bacteria associated with the toxic dinoflagellate *Gymnodinium catenatum*. *J Am Chem Soc* 129(3): 478-479. <https://doi.org/10.1021/ja067369u>
148. Butler A, Theisen RM. 2010. Iron(III)–siderophore coordination chemistry: reactivity of marine siderophores. *Coord Chem Rev* 254(3-4): 288-296. <https://doi.org/10.1016/j.ccr.2009.09.010>
149. Yamamoto S, Okujo N, Yoshida T, Matsuura S, Shinoda S. 1994. Structure and iron transport activity of vibrioferrin, a new siderophore of *Vibrio parahaemolyticus*. *J Biochem* 115(5): 868-874. <https://doi.org/10.1093/oxfordjournals.jbchem.a124432>
150. Shinozaki Y, Kitamoto H, Sameshima-Yamashita Y, Kinoshita A, Nakajima-Kambe T. 2019. Isolation of a novel Co²⁺-resistant bacterium and the application of its siderophore in Co²⁺ recovery from an aqueous solution. *J Gen Appl Microbiol* 65(6): 273-276. <https://doi.org/10.2323/jgam.2018.12.001>
151. Das N, Chandran P. 2011. Microbial degradation of petroleum hydrocarbon contaminants: an overview. *Biotechnol Res Int* 2011: 941810. <https://doi.org/10.4061/2011/941810>
152. Lastochkina O, Pusenkova L, Yuldashev R, Babaev M, Garipova S, et al. 2017. Effects of *Bacillus subtilis* on some physiological and biochemical parameters of *Triticum aestivum* L. (wheat) under salinity. *Plant Physiol Biochem* 121: 80-88. <https://doi.org/10.1016/j.plaphy.2017.10.020>
153. Kalhor SM, Aliniaieifard S, Seif M, Javadi E, Bernard F, et al. 2017. Rhizobacterium *Bacillus subtilis* reduces toxic effects of high electrical conductivity in soilless culture of lettuce. In International Symposium on New Technologies for Environment Control, Energy-Saving and Crop Production in Greenhouse and Plant, Beijing, China.

154. Van Loon LC. 2007. Plant Responses to Plant Growth-promoting Rhizobacteria. In Bakker PAHM, Raaijmakers JM, Bloemberg G, Höfte M, Lemanceau P, et al. (eds) *New Perspectives and Approaches in Plant Growth-Promoting Rhizobacteria Research*. Springer, Dordrecht, pp 243-254.
155. Omidvari M, Sharifi RA, Ahmadzadeh M, Dahaji PA. 2010. Role of fluorescent pseudomonads siderophore to increase bean growth factors. *J Agric Sci* 2(3): 242.
156. Gamalero E, Glick BR. 2011. Mechanisms Used by Plant Growth-Promoting Bacteria. In Maheshwari D (eds) *Bacteria in Agrobiolology: Plant Nutrient Management*. Springer, Berlin, Heidelberg, pp 17-46.
157. Kloepper JW, Leong J, Teintze M, Schroth MN. 1980. Enhanced plant growth by siderophores produced by plant growth-promoting rhizobacteria. *Nature* 286(5776): 885-886. <https://doi.org/10.1038/286885a0>
158. Ghosh SK, Bera T, Chakrabarty AM. 2020. Microbial siderophore – a boon to agricultural sciences. *Biol Control* 144: 104214. <https://doi.org/10.1016/j.biocontrol.2020.104214>
159. Masalha J, Kosegarten H, Elmaci Ö, Mengel K. 2000. The central role of microbial activity for iron acquisition in maize and sunflower. *Biol Fertil Soils* 30: 433-439. <https://doi.org/10.1007/s003740050021>
160. Rungin S, Indananda C, Suttiviriya P, Kruasuwan W, Jaemsang R, et al. 2012. Plant growth enhancing effects by a siderophore-producing endophytic streptomycete isolated from a Thai jasmine rice plant (*Oryza sativa* L. cv. KDML105). *Antonie van Leeuwenhoek* 102: 463-472. <https://doi.org/10.1007/s10482-012-9778-z>
161. Qi W, Zhao L. 2013. Study of the siderophore-producing *Trichoderma asperellum* Q1 on cucumber growth promotion under salt stress. *J Basic Microbiol* 53(4): 355-364. <https://doi.org/10.1002/jobm.201200031>
162. Marschner H, Römheld V, Kissel M. 1986. Different strategies in higher plants in mobilization and uptake of iron. *J Plant Nutr* 9(3-7): 695-713. <https://doi.org/10.1080/01904168609363475>
163. Beneduzi A, Ambrosini A, Passaglia LM. 2012. Plant growth-promoting rhizobacteria (PGPR): their potential as antagonists and biocontrol agents. *Genet Mol Biol* 35: 1044-1051. <https://doi.org/10.1590/S1415-47572012000600020>
164. Schippers B, Bakker AW, Bakker PA. 1987. Interactions of deleterious and beneficial rhizosphere microorganisms and the effect of cropping practices. *Annu Rev Phytopathol* 25(1): 339-358. <https://doi.org/10.1146/annurev.py.25.090187.002011>
165. Voisard C, Keel C, Haas D, Dèfago G. 1989. Cyanide production by *Pseudomonas fluorescens* helps suppress black root rot of tobacco under gnotobiotic conditions. *EMBO J* 8(2): 351-358. <https://doi.org/10.1002/j.1460-2075.1989.tb03384.x>
166. Pal KK, Tilak KVBR, Saxena AK, Dey R, Singh CS. 2001. Suppression of maize root diseases caused by *Macrophomina phaseolina*, *Fusarium moniliforme* and *Fusarium graminearum* by plant growth promoting rhizobacteria. *Microbiol Res* 156(3): 209-223. <https://doi.org/10.1078/0944-5013-00103>
167. Yu X, Ai C, Xin L, Zhou G. 2011. The siderophore-producing bacterium, *Bacillus subtilis* CAS15, has a biocontrol effect on Fusarium wilt and promotes the growth of pepper. *Eur J Soil Biol* 47(2): 138-145. <https://doi.org/10.1016/j.ejsobi.2010.11.001>
168. Verma VC, Singh SK, Prakash S. 2011. Bio-control and plant growth promotion potential of siderophore producing endophytic *Streptomyces* from *Azadirachta indica* A. Juss. *J Basic Microbiol* 51(5): 550-556. <https://doi.org/10.1002/jobm.201000155>
169. Hamdan H, Weller DM, Thomashow LS. 1991. Relative importance of fluorescent siderophores and other factors in biological control of *Gaeumannomyces graminis* var. *tritici* by *Pseudomonas fluorescens* 2-79 and M4-80R. *Appl Environ Microbiol* 57(11): 3270-3277. <https://doi.org/10.1128/aem.57.11.3270-3277.1991>
170. McLoughlin TJ, Quinn JP, Bettermann A, Bookland R. 1992. *Pseudomonas cepacia* suppression of sunflower wilt fungus and role of antifungal compounds in controlling the disease. *Appl Environ Microbiol* 58(5): 1760-1763. <https://doi.org/10.1128/aem.58.5.1760-1763.1992>
171. Velidandi A, Dahariya S, Pabbathi NPP, Kalivarathan D, Baadhe RR. 2020. A review on synthesis, applications, toxicity, risk assessment and limitations of plant extracts synthesized silver nanoparticles. *NanoWorld J* 6(3): 35-60. <https://doi.org/10.17756/nwj.2020-079>
172. Velidandi A, Pabbathi NPP, Dahariya S, Baadhe RR. 2020. Catalytic and eco-toxicity investigations of bio-fabricated monometallic nanoparticles along with their anti-bacterial, anti-inflammatory, anti-diabetic, anti-oxidative and anti-cancer potentials. *Colloid Interface Sci Commun* 38: 100302. <https://doi.org/10.1016/j.colcom.2020.100302>
173. Vankdoth S, Velidandi A, Sarvepalli M, Vangalapati M. 2022. Poly-extract synthesized silver nanoparticles catalysed rhodamine-B and methyl orange dye degradation: influence of physicochemical parameters and their recyclability. *NanoWorld J* 8(2): 42-54. <https://doi.org/10.17756/nwj.2022-099>
174. Velidandi A, Pabbathi NPP, Baadhe RR. 2021. Study of parameters affecting the degradation of rhodamine-B and methyl orange dyes by *Annona muricata* leaf extract synthesized nanoparticles as well as their recyclability. *J Mol Struct* 1236: 130287. <https://doi.org/10.1016/j.molstruc.2021.130287>
175. Khatoun UT, Velidandi A, Rao NGVS. 2024. Nano-sized copper particles: chemical synthesis, characterization, and their size and surface charge dependent antibacterial potential. *Results Chem* 7: 101258. <https://doi.org/10.1016/j.rechem.2023.101258>
176. Velidandi A, Sarvepalli M, Gandam PK, Baadhe RR. 2023. Silver/silver chloride and gold bimetallic nanoparticles: green synthesis using *Azadirachta indica* aqueous leaf extract, characterization, antibacterial, catalytic, and recyclability studies. *Inorg Chem Commun* 155: 111107. <https://doi.org/10.1016/j.inoche.2023.111107>
177. Sarvepalli M, Korrapati N. 2023. Statistical optimisation of process parameters involved in siderophore production of marine bacterial isolate *Marinobacter* sp. SVU_3. *Biomass Convers Biorefinery* 1-12. <https://doi.org/10.1007/s13399-023-04427-y>
178. Sarvepalli M, Velidandi A, Korrapati N. 2023. Optimization of siderophore production in three marine bacterial isolates along with their heavy-metal chelation and seed germination potential determination. *Microorganisms* 11(12): 2873. <https://doi.org/10.3390/microorganisms11122873>
179. Klitsche F, Ramcke J, Migenda J, Hensel A, Vossmeier T, et al. 2015. Synthesis of tripodal catecholates and their immobilization on zinc oxide nanoparticles. *Beilstein J Org Chem* 11(1): 678-686. <http://doi.org/10.3762/bjoc.11.77>
180. Galinetto P, Taglietti A, Pasotti L, Pallavicini P, Dacarro G, et al. 2016. SERS activity of silver nanoparticles functionalized with a desferrioxamine B derived ligand for Fe(III) binding and sensing. *J Appl Spectrosc* 82: 1052-1059. <https://doi.org/10.1007/s10812-016-0228-y>
181. Wyatt MA, Johnston CW, Magarvey NA. 2014. Gold nanoparticle formation via microbial metallophore chemistries. *J Nanopart Res* 16: 2212. <https://doi.org/10.1007/s11051-013-2212-2>
182. Barsainya M, Singh DP. 2018. Green synthesis of zinc oxide nanoparticles by *Pseudomonas aeruginosa* and their broad-spectrum antimicrobial effects. *J Pure Appl Microbiol* 12(4): 2123-2134. <http://doi.org/10.22207/JPAM.12.4.50>
183. Patil S, Sastry M, Bharde A. 2022. Size and shape directed novel green synthesis of plasmonic nanoparticles using bacterial metabolites and their anticancer effects. *Front Microbiol* 13: 866849. <https://doi.org/10.3389/fmicb.2022.866849>
184. Martínez-Matamoros D, Castro-García S, Balado M, Matamoros-Veloz A, Camargo-Valero MA, et al. 2019. Preparation of functionalized magnetic nanoparticles conjugated with feroxamine and their evaluation for pathogen detection. *RSC Adv* 9(24): 13533-13542. <https://doi.org/10.1039/c8ra10440a>
185. Phillips DJ, Davies GL, Gibson MI. 2015. Siderophore-inspired nanoparticle-based biosensor for the selective detection of Fe³⁺. *J Mater Chem B* 3(2): 270-275. <https://doi.org/10.1039/c4tb01501k>

186. Kumari R, Barsainya M, Singh DP. 2017. Biogenic synthesis of silver nanoparticle by using secondary metabolites from *Pseudomonas aeruginosa* DM1 and its anti-algal effect on *Chlorella vulgaris* and *Chlorella pyrenoidosa*. *Environ Sci Pollut Res* 24: 4645-4654. <https://doi.org/10.1007/s11356-016-8170-3>
187. Laisney J, Chevallet M, Fauquant C, Sageot C, Moreau Y, et al. 2022. Ligand-promoted surface solubilization of TiO₂ nanoparticles by the enterobactin siderophore in biological medium. *Biomolecules* 12(10): 1516. <https://doi.org/10.3390/biom12101516>
188. Khatoon UT, Velidandi A, Nageswara Rao GVS. 2024. Silver oxide nanoparticles: synthesis via chemical reduction, characterization, antimicrobial, and cytotoxicity studies. *Inorg Chem Commun* 159: 111690. <https://doi.org/10.1016/j.inoche.2023.111690>
189. Khatoon UT, Velidandi A, Nageswara Rao GVS. 2023. Copper oxide nanoparticles: synthesis via chemical reduction, characterization, antibacterial activity, and possible mechanism involved. *Inorg Chem Commun* 149: 110372. <https://doi.org/10.1016/j.inoche.2022.110372>
190. Khatoon UT, Velidandi A, Nageswara Rao GVS. 2023. Sodium borohydride mediated synthesis of nano-sized silver particles: their characterization, anti-microbial and cytotoxicity studies. *Mater Chem Phys* 294: 126997. <https://doi.org/10.1016/j.matchemphys.2022.126997>
191. Frei A, Verderosa AD, Elliott AG, Zuegg J, Blaskovich MA. 2023. Metals to combat antimicrobial resistance. *Nat Rev Chem* 7(3): 202-224. <https://doi.org/10.1038/s41570-023-00463-4>
192. Velidandi A, Sarvepalli M, Gandam PK, Pabbathi NPP, Baadhe RR. 2023. Characterization, catalytic, and recyclability studies of nano-sized spherical palladium particles synthesized using aqueous poly-extract (turmeric, neem, and tulasi). *Environ Res* 228: 115821. <https://doi.org/10.1016/j.envres.2023.115821>
193. Velidandi A, Sarvepalli M, Aramanda P, Amudala ML, Baadhe RR. 2023. Effect of size on physicochemical, antibacterial, and catalytic properties of *Neolamarckia cadamba* (burflower-tree) synthesized silver/silver chloride nanoparticles. *Environ Sci Pollut Res* 30(22): 63231-63249. <https://doi.org/10.1007/s11356-023-26427-1>
194. Breijyeh Z, Karaman R. 2023. Design and synthesis of novel antimicrobial agents. *Antibiotics* 12(3): 628. <https://doi.org/10.3390/antibiotics12030628>
195. Velidandi A, Pabbathi NPP, Dahariya S, Baadhe RR. 2021. Green synthesis of novel Ag-Cu and Ag-Zn bimetallic nanoparticles and their *in vitro* biological, eco-toxicity and catalytic studies. *Nano Struct Nano Objects* 26: 100687. <https://doi.org/10.1016/j.nanos.2021.100687>
196. Velidandi A, Pabbathi NPP, Dahariya S, Kagithoju S, Baadhe RR. 2022. Bio-fabrication of silver-silver chloride nanoparticles using *Annona muricata* leaf extract: characterization, biological, dye degradation and eco-toxicity studies. *Int J Environ Sci Technol* 19(7): 6555-6572. <https://doi.org/10.1007/s13762-021-03461-5>
197. Vankdoth S, Velidandi A, Sarvepalli M, Vangalapati M. 2022. Role of plant (tulsi, neem and turmeric) extracts in defining the morphological, toxicity and catalytic properties of silver nanoparticles. *Inorg Chem Commun* 140: 109476. <https://doi.org/10.1016/j.inoche.2022.109476>
198. Velidandi A, Sarvepalli M, Pabbathi NPP, Baadhe RR. 2021. Biogenic synthesis of novel platinum-palladium bimetallic nanoparticles from aqueous *Annona muricata* leaf extract for catalytic activity. *3 Biotech* 11(8): 385. <https://doi.org/10.1007/s13205-021-02935-0>
199. Kotb E, Ahmed AA, Saleh TA, Ajeebi AM, Al-Gharsan MS, et al. 2020. Pseudobactins bounded iron nanoparticles for control of an antibiotic-resistant *Pseudomonas aeruginosa* rym32. *Biotechnol Prog* 36(1): e2907. <https://doi.org/10.1002/btpr.2907>
200. Makvandi P, Wang CY, Zare EN, Borzacchiello A, Niu LN, et al. 2020. Metal-based nanomaterials in biomedical applications: antimicrobial activity and cytotoxicity aspects. *Adv Funct Mater* 30(22): 1910021. <https://doi.org/10.1002/adfm.201910021>
201. Franco D, Calabrese G, Guglielmino SPP, Conoci S. 2022. Metal-based nanoparticles: antibacterial mechanisms and biomedical application. *Microorganisms* 10(9): 1778. <https://doi.org/10.3390/microorganisms10091778>
202. Nosrati R, Abnous K, Alibolandi M, Mosafar J, Dehghani S, et al. 2021. Targeted SPION siderophore conjugate loaded with doxorubicin as a theranostic agent for imaging and treatment of colon carcinoma. *Sci Rep* 11(1): 13065. <https://doi.org/10.1038/s41598-021-92391-w>
203. Salek Maghsoudi A, Hassani S, Mirnia K, Abdollahi M. 2021. Recent advances in nanotechnology-based biosensors development for detection of arsenic, lead, mercury, and cadmium. *Int J Nanomed* 16: 803-832. <https://doi.org/10.2147/IJN.S294417>
204. Wang Z, Wang H, Cheng X, Geng J, Wang L, et al. 2021. Aptamer-superparamagnetic nanoparticles capture coupling siderophore-Fe³⁺ scavenging actuated with carbon dots to confer an "off-on" mechanism for the ultrasensitive detection of *Helicobacter pylori*. *Biosens Bioelectron* 193: 113551. <https://doi.org/10.1016/j.bios.2021.113551>
205. Camara-Martos F, da Costa J, Justino CI, Cardoso S, Duarte AC, et al. 2016. Disposable biosensor for detection of iron(III) in wines. *Talanta* 154: 80-84. <https://doi.org/10.1016/j.talanta.2016.03.057>